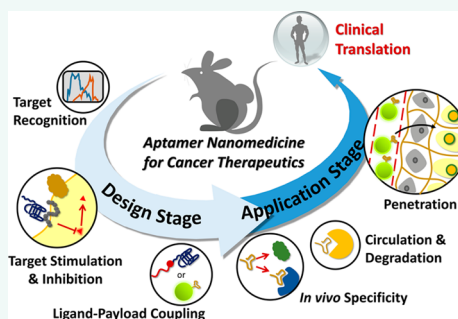


# Aptamer Nanomedicine for Cancer Therapeutics: Barriers and Potential for Translation

Yeh-Hsing Lao,<sup>†</sup> Kyle K.L. Phua,<sup>‡</sup> and Kam W. Leong<sup>\*†</sup>

<sup>†</sup>Department of Biomedical Engineering, Columbia University, New York 10027, New York, United States and <sup>‡</sup>Department of Chemical & Biomolecular Engineering, National University of Singapore, Singapore 117585

**ABSTRACT** Aptamer nanomedicine, including therapeutic aptamers and aptamer nanocomplexes, is beginning to fulfill its potential in both clinical trials and preclinical studies. Especially in oncology, aptamer nanomedicine may perform better than conventional or antibody-based chemotherapeutics due to specificity compared to the former and stability compared to the latter. Many proof-of-concept studies on applying aptamers to drug delivery, gene therapy, and cancer imaging have shown promising efficacy and impressive safety *in vivo* toward translation. Yet, there remains ample room for improvement and critical barriers to be addressed. In this review, we will first introduce the recent progress in clinical trials of aptamer nanomedicine, followed by a discussion of the barriers at the design and *in vivo* application stages. We will then highlight recent advances and engineering strategies proposed to tackle these barriers. Aptamer cancer nanomedicine has the potential to address one of the most important healthcare issues of the society.



**KEYWORDS:** aptamer · nanomedicine · SELEX · clinical trial · cancer therapy · drug delivery · gene therapy · *in vivo* imaging

An aptamer is a short oligonucleotide that can fold into a unique tertiary structure that recognizes a specific target ranging from small organic molecules to proteins to cells.<sup>1–3</sup> It is generated from an evolutionary selection method, systematic evolution of ligands by exponential enrichment (SELEX), first established in the 1990s.<sup>4,5</sup> Since then, the aptamer has become a notable class of targeting ligand for both diagnostics<sup>6–8</sup> and therapeutics.<sup>9–11</sup> In general, the aptamer acts in a manner similar to that of an antibody, but it may have advantages in therapeutic applications, especially in the field of oncology. Compared with an antibody, the aptamer does not have an Fc region, which interacts with soluble Fc receptors<sup>12</sup> or Fc receptors expressed on immune cells and other certain types of cells.<sup>13,14</sup> This obviates undesired interaction in systemic administration, which may result in immune stimulation or other unforeseen side effects. Also, for the treatment of solid tumors, an antibody's high molecular weight impedes its ability to penetrate into the deep site of the tumor.

In contrast, the molecular weight of the aptamer is usually in the range between 6 and 30 kDa, much smaller than that of the antibody (~150 kDa), which results in better tumor uptake kinetics.<sup>15</sup> Moreover, the aptamer has higher stability than the protein in biological fluids and lower production costs. Thus, the aptamer is attractive as a cancer therapeutic component. Importantly, the mature synthesis technology of nucleic acid facilitates the design of an aptamer with any sequence and structure to suit diverse applications. Currently, there is one aptamer available in the clinic and 10 under clinical trials. The aptamer specifically recognizing human vascular endothelial growth factor (VEGF) has been approved for the treatment of age-related macular degeneration (AMD) in the U.S. and the EU.<sup>16</sup> Aptamers for other applications in coagulation, oncology, and inflammation have also shown therapeutic efficacy in clinical trials.

Cancer therapy demands more effective therapeutics, particularly targeted therapeutics, to spare normal cells from toxicity.

\* Address correspondence to kam.leong@columbia.edu.

Received for review December 31, 2014 and accepted March 3, 2015.

Published online March 03, 2015  
10.1021/nn507494p

© 2015 American Chemical Society

As mentioned above, the aptamer is an antibody alternative with fewer limitations associated with the intrinsic properties of an antibody.<sup>1</sup> As a result, aptamer nanomedicine (therapeutic aptamers and aptamer nanocomplexes) possesses great potential for cancer treatment, and a variety of promising aptamer nanomedicine systems have been reported for drug therapy, gene therapy, and tumor imaging. *In vivo* results from these studies are promising, but critical issues, such as stability, functionality, and robustness, must be addressed for translation.

These critical issues give rise to challenges at both stages of design and *in vivo* application of aptamer nanomedicine, as shown in Figure 1. At the design stage, major barriers are associated with aptamer selection. Conventional SELEX technology is unable to generate an aptamer against certain targets. How to obtain a high-affinity aptamer for target recognition is the first and the most important issue. Once the aptamer is obtained, the next question is whether this aptamer is capable of stimulating or inhibiting the target's functionality. Typically, an aptamer is expected to bind like a monoclonal antibody and possess a therapeutic function, such as inhibition of tumor growth. With this consideration, a majority of aptamers discovered so far are not functional, so "upgrading" the aptamer with a therapeutic payload to interfere with the target's functionality will be important for therapy. Nanotechnology also enables researchers to couple different therapeutic payloads to aptamers, leading to the development of aptamer nanocomplexes.

At the application stage, navigation across biological barriers with specificity is crucial. Off-target effects should be assessed during the process of aptamer selection, and modifications can be made before *in vivo* assessment. A variety of modifications can prevent nuclease-mediated degradation and prolong systemic circulation to increase the chance of aptamer nanomedicine reaching the tumor tissue. Yet, they may

**VOCABULARY: Aptamer** - a synthetic oligonucleotide that can specifically and strongly bind to a specific target; **SELEX** - an artificially, iteratively evolutionary process to generate highly specific aptamers. To perform SELEX, a DNA or an RNA library is first incubated with the target. Candidates that specifically interact with the target are obtained when candidates that bind to targets are eluted and subsequently amplified to generate a new pool for the next round of selection; **Aptamer nanocomplex** - a drug or a nanoparticle conjugated with aptamers to enhance the specificity of targeting; **Aptamer chimera** - an oligonucleotide composed of an aptamer for targeting and a therapeutic nucleic acid for treatment;

still face the obstacle of penetrating the tumor microvessels into the tumor core. In this review, we will first introduce the current status of aptamer nanomedicine in clinical trials. Next we will discuss the major barriers to aptamer nanomedicine at the design and application stages and highlight the advances that address these issues in the preclinical pipeline (Table 1). We will also speculate on the future trajectory of these advances and illustrate the potential translation route for aptamer nanomedicine.

## APTAMER NANOMEDICINE IN CLINICS AND CLINICAL TRIALS

To date, 11 aptamers are under clinical trials (one for AMD has been approved) for treatments related to macular degeneration, coagulation, oncology, and inflammation (Figure 2). In this section, we will review the application of these aptamers in the treatment of each disease.

**Age-Related Macular Degeneration.** Among those under clinical evaluation, aptamers for the treatment of AMD have made remarkable advances (Figure 2A). Approximately, 8 million Americans suffer from two major types of AMD, namely, neovascular (wet) and atrophic (dry) AMD.<sup>17</sup> Wet and dry AMDs occur due to choroidal

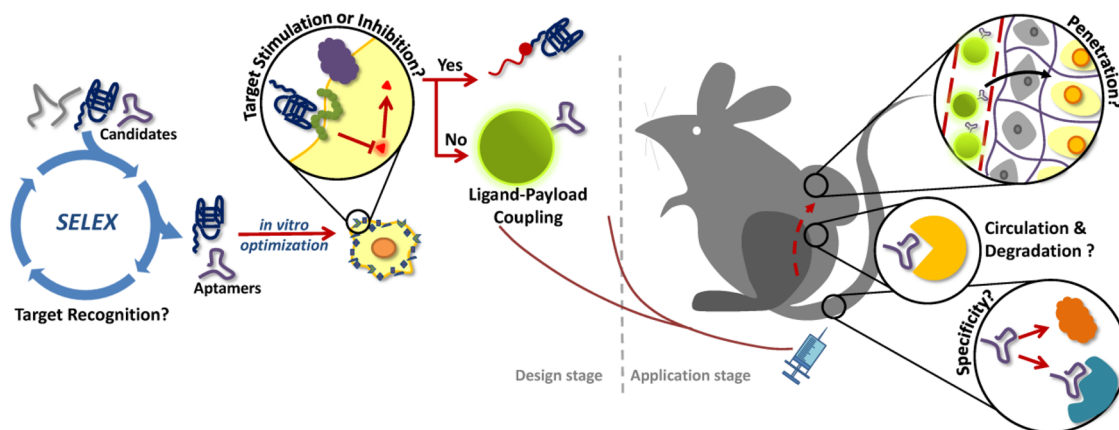


**Figure 1.** Barriers at the design and *in vivo* application stages for the development of aptamer cancer nanomedicine. Target recognition, target inhibition/stimulation, and ligand–payload coupling are major barriers at the design stage. When applied *in vivo*, cell and tissue specificity, immunogenicity, degradation, systemic circulation, and tumor penetration are the important barriers.

**TABLE 1. Summary of Selected Aptamer Cancer Nanomedicine Systems in the Preclinical Pipeline**

application	target	aptamer		sequence modification	payload	carrier	loading and preparation strategy	ref
		type	$K_D$ (nM)					
drug delivery	prostate-specific membrane antigen (PSMA)	RNA	11.9 <sup>69,a</sup>	none	doxorubicin	hyper-branched polyester core with a PEG–PLA shell	hydrophobic interaction	68
	PSMA	RNA	11.9 <sup>69,a</sup>	2'-F-modifications	docetaxel	PEG–PLGA nanoparticle (NP)	nanoprecipitation	70
	PSMA	RNA	11.9 <sup>69,a</sup>	2'-F-modifications 3'-inverted T cap	Pt(IV) prodrug	PEG–PLGA NP	nanoprecipitation	71
	protein tyrosine kinase-7 (PTK-7)	DNA	0.8 <sup>64</sup>	none	doxorubicin	additional DNA duplexes	intercalation	72
	nucleolin	DNA	n/a <sup>b</sup>	none	paclitaxel	PEG–PLGA NP	emulsion/solvent evaporation	61
	nucleolin	DNA	n/a <sup>b</sup>	none	doxorubicin	liposome	hydration/extrusion	74
gene therapy	PSMA	RNA	11.9 <sup>69,a</sup>	2'-F-modifications	PLK1, BCL2 siRNAs	none	chimera	80
	PSMA	RNA	11.9 <sup>69,a</sup>	2'-F-modifications	DNAPK shRNA	none	chimera	84
	PSMA	RNA	11.9 <sup>69,a</sup>	none	AR shRNA construct	PEG–PLGA NP	solvent displacement	93
	Axl receptor tyrosine kinase	RNA	12 <sup>91</sup>	2'-F-modifications	let-7g miRNA	none	chimera	96
	nucleolin	DNA	n/a <sup>b</sup>	none	SLUG, NRP1 siRNAs	none	chimera	87
	nucleolin	DNA	n/a <sup>b</sup>	none	BRAF siRNA	liposome	lipoplex formation	85
imaging	mucin 1 (MUC-1)	DNA	0.135 <sup>88</sup>	none	mi-29b miRNA	none	chimera	97
	tenascin-C	RNA	5 <sup>110</sup>	2'-OMe and 2'-F-modifications 3'-inverted T cap PEGylation	<sup>99m</sup> Tc chelate complex	none	direct conjugation	90
	Ramos cell line	DNA	74.7 <sup>98</sup>	none	Cy5	none	direct conjugation	15
	PTK-7	DNA	0.8 <sup>64</sup>	none	Cy5/BHQ2	none	direct conjugation	100
	nucleolin	DNA	n/a <sup>b</sup>	none	silica-coated Mn <sub>3</sub> O <sub>4</sub> NP	none	direct conjugation	105
	VEGF receptor 2	DNA	0.12	modified bases <sup>c</sup>	SPION	none	direct conjugation	107
	neutrophil elastase	DNA	n/a <sup>b</sup>	none	<sup>99m</sup> Tc chelate complex	none	direct conjugation	108
	MUC-1	DNA	0.135 <sup>88</sup>	none	<sup>99m</sup> Tc chelate complex	none	direct conjugation	109
	MUC-1	DNA	0.135 <sup>88</sup>	none	SPION + epirubicin	additional DNA duplexes (drug)	direct conjugation (SPION) + intercalation (drug)	111
	MUC-1	DNA	0.135 <sup>88</sup>	none	quantum dot + doxorubicin	none	direct conjugation	113
immunotherapy	cytotoxic T cell antigen-4 (CTLA4)	RNA	33 <sup>139</sup>	2'-F-modifications	Anti-CTLA4 aptamers	none	tetramerization	114
	CTLA4	RNA	33 <sup>139</sup>	n/a <sup>b</sup>	STAT3 siRNA	none	chimera	139

<sup>a</sup> Reported as an enzyme inhibition constant ( $K_i$ ). <sup>b</sup> Information not available. <sup>c</sup> 5-N-(Benzylcarboxamide)-2'-deoxyuridine (BzdU).

neovascularization and degeneration of retinal pigment epithelial cells, respectively. Pegaptanib (Macugen; Pfizer and Eyetech), which is approved for wet AMD treatment, is an RNA aptamer that specifically recognizes human VEGF.<sup>16</sup> VEGF promotes angiogenesis and is often up-regulated under certain conditions (e.g., wound healing) or diseases (e.g., wet AMD).<sup>18</sup> Pegaptanib binds to the heparin-binding site of VEGF and blocks the interaction between VEGF and its receptors, which results in the prevention or reduction of the neovascularization. In 2004, pegaptanib became the first antiangiogenesis drug for wet AMD therapy under intravitreal administration with a dosage of 0.3 mg per eye every 6 weeks.<sup>16</sup> However, pegaptanib only recognizes the abundant isoform of VEGF, VEGF<sub>165</sub>, whereas ranibizumab (Lucentis; Genentech), an antibody competitor developed later, can bind to all isoforms of VEGF.<sup>19</sup> Nevertheless, recent results of the phase IV clinical trial indicate that pegaptanib may be a safer option for the long-term maintenance therapy.<sup>20</sup> This is because VEGF also regulates blood pressure in addition to angiogenesis, and blocking all the VEGFs may

increase the risk of hypertension and other side effects, especially for patients with systemic comorbidities.<sup>21</sup> Hence, for these patients, pegaptanib would be suitable as boosters to improve the visual acuity for long-term treatment of wet AMD.

Anti-VEGF therapy alone may not be sufficient for the new vessel regression to prevent angiogenesis due to the influence of vessel maturation, which is associated with pericytes. Platelet-derived growth factor (PDGF) plays a role in pericyte recruitment and causes new vessels to become resistant to anti-VEGF drugs.<sup>22,23</sup> An *in vivo* study demonstrates that the combination of pegaptanib and anti-PDGF antibody can not only prevent neovascularization but also cause vessel regression.<sup>23</sup> An anti-PDGF aptamer, E10030 (Fovista; Ophthotech), was developed and optimized from a DNA-based SELEX<sup>24</sup> for similar purposes. Now, a combinational therapy comprising E10030 and ranibizumab awaits phase III evaluation for wet AMD treatment (clinical trial IDs NCT01944839 and NCT01940900). Ophthotech has another RNA aptamer (ARC1905) against complement component 5 (C5) also

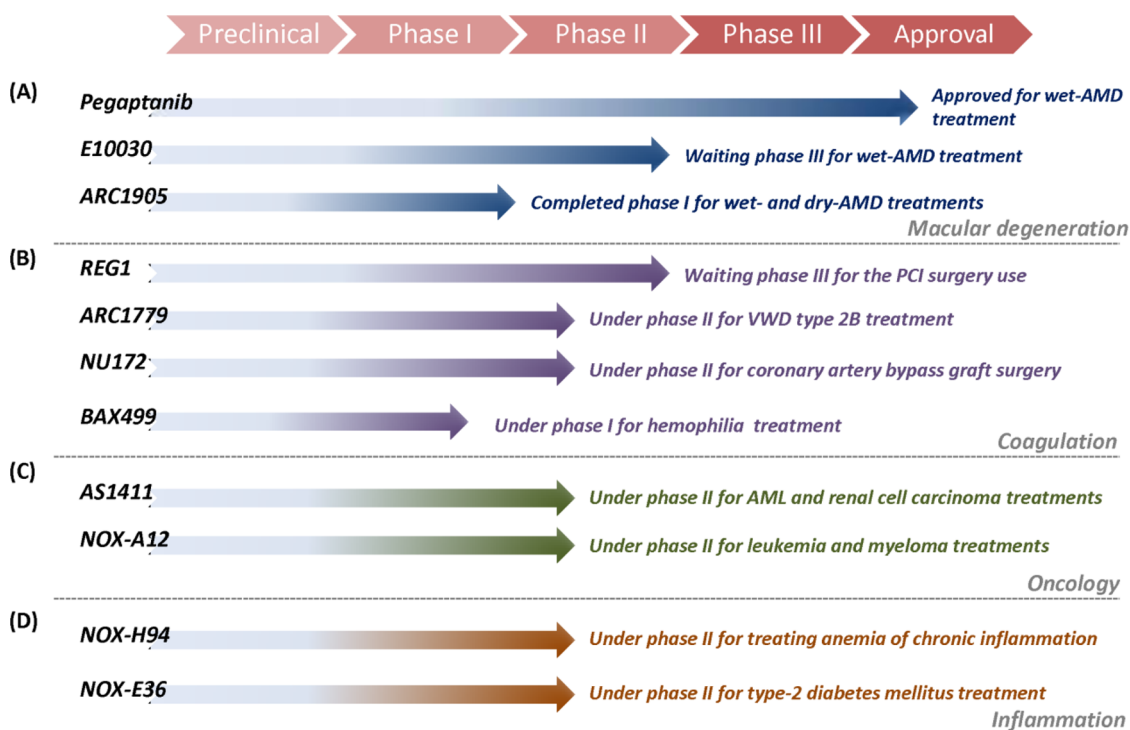


Figure 2. Current progress of aptamer nanomedicine for (A) macular degeneration, (B) coagulation, (C) oncology, and (D) inflammation in clinical trials.

under development for AMD treatment.<sup>25</sup> C5 is a downstream protein in the complement cascade reportedly associated with the pathogenesis of AMD.<sup>26</sup> Thus, C5 may be a therapeutic target for both wet and dry AMDs. Ophthotech has recently completed phase I clinical trials using ARC1905 for these two types of AMDs (clinical trial IDs NCT00709527 and NCT00950638).

**Coagulation.** Coagulation is another significant clinical application for aptamers. There are four aptamers now in clinical trials (Figure 2B). The first aptamer, REG1 (Regado Biosciences),<sup>27</sup> has recently passed phase II clinical trials for its use in the surgery of percutaneous coronary intervention (PCI) for patients with coronary artery disease (clinical trial ID NCT00715455). This system comprises a 37-mer RNA aptamer RB006 (Pegnivacogin) and an antidote RB007 (Anivamersen), which is a 17-mer complementary sequence of RB006.<sup>27</sup> RB006 acts as an antagonist against factor IXa to prevent the downstream conversion of factor X and prolongs clotting time. RB007 can specifically reverse the functionality of RB006, so the sheath removal time after PCI can be well controlled by the dose of RB007. Compared with the currently available anticoagulation/antidote pair (heparin/protamine), the REG1 system is less toxic, and the therapeutic effects can be precisely controlled by adjustment of dosage.<sup>28</sup>

The second aptamer is ARC1779 (Baxter),<sup>29</sup> which binds to von Willebrand factor (VWF), a key factor in the coagulation cascade associated with platelet recruitment. If this protein is deficient or defective, the clotting cascade will malfunction and result in bleeding

disorders known as von Willebrand diseases (VWD).<sup>30</sup> The type 2B VWD is one subclass of this disease associated with a mutated VWF, which shows higher affinity against platelets compared with normal VWF. Since mutation of VWF does not influence multimer formation and digestion, mutated VWF multimers would spontaneously interact with platelets and can be cleaved by ADAMTS-13 enzyme. Consequently, small VWF multimer–platelet complexes would reduce the efficiency of platelet adhesion and boost the clearance rate of the complexes and cause symptoms such as thrombocytopenia.<sup>31</sup> Aptamer ARC1779 is a DNA aptamer that recognizes VWF's A1 domain, which binds to the glycoprotein 1b of the platelet.<sup>29</sup> This aptamer can block spontaneous interaction between VWF and platelets. A recent phase II pilot study shows that ARC1779 can effectively prevent desmopressin (a VWF agonist)-induced platelet depletion in the patients treated with ARC1779 and desmopressin by inhibiting the VWF–platelet interaction.<sup>32</sup>

The third aptamer is NU172 (ARCA Biopharma),<sup>33</sup> designed as a short-term anticoagulant and distinct from REG1 and ARC1779. It is an unmodified DNA aptamer recognizing the exosite I of thrombin. NU172 can effectively prolong the clotting time in preclinical studies, and the anticoagulation function is rapidly terminated due to its degradation. A phase II clinical trial designed for the application of this aptamer in coronary artery bypass graft surgery is under consideration (clinical trial ID NCT00808964).

Unlike other aptamers targeting the proteins in the intrinsic coagulation pathway, the fourth aptamer

BAX499 (formerly known as ARC19499; Baxter)<sup>34</sup> interacts with the tissue factor pathway inhibitor, which is a negative regulator of factor VIIa in the extrinsic pathway. In a preclinical monkey model, BAX499 can restore the clotting defect induced by the antifactor VIII antibody, which mimics the pathology of hemophilia. It entered phase I clinical trials in 2010, and the results are pending (clinical trial ID NCT01191372).

**Oncology.** In the field of oncology (Figure 2C), two aptamers, namely, AS1411<sup>35</sup> and NOX-A12,<sup>36</sup> have entered clinical trials. AS1411 (formerly ARG0100; Antisoma)<sup>35</sup> is a guanine quadruplex aptamer obtained from a guanine-rich oligonucleotide library in the antiproliferation screen, which is not a typical SELEX process. The guanine quadruplex structure benefits AS1411 because it is resistant to nuclease degradation and enhances cell uptake. In *in vitro* validations, AS1411 inhibits more than 80 types of cancer cell lines. In addition, the target of AS1411 has been verified to be nucleolin, and the relevant mechanism and specificity against cancer cells have also been described. In preclinical tests, AS1411 shows efficacy toward xenograft models, including non-small cell lung, renal, and breast cancers. It entered clinical trials in 2003 and passed phase II trials for acute myeloid leukemia. A subsequent phase II trial for renal cell carcinoma started in 2008 (clinical trial ID NCT00740441). NOX-A12 (Olaptesed pegol; Noxxon)<sup>36</sup> is an L-form RNA aptamer known as Spiegelmer<sup>37</sup> and is used for cancer therapy. NOX-A12 targets the chemokine CXCL-12 and blocks its binding to its receptor.<sup>36</sup> This disrupts the tissue gradient of CXCL-12 and reduces the cancer cell homing that might lead to tumor metastasis and drug resistance.<sup>38</sup> Currently, phase II clinical trials for NOX-A12 are underway for the treatment of chronic lymphocytic leukemia and refractory multiple myeloma (clinical trial IDs NCT01486797 and NCT01521533).

**Inflammation.** Two other Spiegelmers, NOX-H94 (Lexaptepid pegol)<sup>39</sup> and NOX-E36 (Emapticap pegol),<sup>40</sup> both from Noxxon, are designed for the treatment of disease-induced inflammation (Figure 2D). NOX-H94 targets hepcidin, a peptide hormone regulating the iron homeostasis, and interferes with the interaction between hepcidin and ferroportin.<sup>39</sup> For patients with chronic inflammation associated with cancer and dialysis, hepcidin is up-regulated and leads to anemia because of hepcidin-induced ferroportin degradation.<sup>41</sup> NOX-H94 can reduce the symptom of anemia caused by chronic inflammation by inhibiting the functionality of hepcidin.<sup>39</sup> In the preclinical study using a *Cynomolgus* monkey model, pretreatment with NOX-H94 can prevent the interleukin-6-induced drop in serum iron concentration. This aptamer initially entered clinical trials for the treatment of anemia caused by chronic inflammation in patients with cancers and completed phase IIa trials recently (clinical ID NCT01691040). Now Noxxon also plans to use NOX-H94 to treat dialysis

patients who have erythropoiesis-stimulating agent-induced anemia, and phase I/II trials (clinical trial ID NCT02079896) have begun. NOX-E36 is another Spiegelmer for inflammation treatment.<sup>40</sup> It recognizes the CC motif chemokine ligand 2 (CCL2; also known as monocyte chemoattractant protein 1, MCP-1), which mediates inflammation *via* leukocyte recruitment from vascular to extravascular space. NOX-E36 prevents CCL2-induced inflammation by binding to CCL2 and thereby reducing leukocyte recruitment. NOX-E36 is effective in the treatment of lupus nephritis<sup>40</sup> and in the prevention of type-2 diabetic glomerulosclerosis<sup>42</sup> in the mice models. This aptamer is currently being evaluated in phase II clinical trials for type-2 diabetic patients (clinical trial IDs NCT01085292 and NCT01547897).

Compared with the current therapeutic strategies, these aptamers in clinical trials are advantageous particularly for safety issues. They also show significant improvement in efficacy. In addition to these aptamers, more aptamer nanomedicine systems are being developed especially for cancer therapy.

#### BARRIERS AT THE DESIGN STAGE FOR APTAMER NANOMEDICINE

At the design stage, SELEX is the most important technique to generate an aptamer that recognizes its desired target. The concept of SELEX was independently demonstrated by Gold's and Szostak's groups in the 1990s.<sup>4,5</sup> The aptamer is screened from a nucleic acid library composed of  $10^{14}$  to  $10^{16}$  different candidates, and each candidate comprises 30–60 random nucleotides between two fixed primers. Due to sequence differences, candidates fold into different secondary and tertiary structures. When candidates are incubated with the target, only those that bind with high affinity against the target can be eluted from the target–candidate complex. The target-specific candidates are amplified either by polymerase chain reaction (PCR) (for DNA aptamer) or by reverse-transcriptase PCR (for RNA aptamer). Subsequently, enriched candidates are activated by single-strand isolation (DNA aptamer) or *in vitro* transcription (RNA aptamer) for the next selection round. Through round-by-round selection, the dissociation constant ( $K_D$ ) of the candidate pool can be improved from micromolar ( $\mu\text{M}$ ) to low nanomolar (nM) or even picomolar (pM) range. Candidates will eventually converge to several representative aptamers that recognize the target with high affinities and specificities. This iterative process continues until the best performing aptamer is obtained from the SELEX process and the resulting aptamer is capable of target recognition. However, the candidates may bind to any epitopes on the target protein in the incubation step, so the conventional SELEX technique cannot ensure that the obtained aptamer binds to a specific epitope of the target, which

may be required for downstream signaling, leading to the desired therapeutic outcome. In other words, aptamer candidates identified through SELEX may not hold the expected ability to stimulate or inhibit the functionality of the target. For this barrier, researchers may need to use either a specialized selection approach to generate an aptamer that can interfere with the target's functionality or a conjugate aptamer with a therapeutic payload to form a nanocomplex for the desired therapeutic outcome.

**Target Recognition.** The dissociation constant between the aptamer and the target is the most important parameter that assists researchers in determining whether SELEX is successful. Generally, the candidate pool's  $K_D$  in the final round of a successful selection should be lower than 30 nM.<sup>43</sup> Although SELEX is theoretically capable of generating a high-affinity aptamer against any target, the success rate of aptamer generation through the conventional SELEX technique is lower than 30%,<sup>43</sup> and conventional SELEX fails in the screening toward some "difficult" proteins. This limitation may be due to a lack of structural diversity of the nucleic acids, which only consists of four building blocks—two pyridines and two purines. Also, the backbone of nucleic acid is highly negative-charged, so the natural aptamer candidates may not interact with some negative-charged proteins. Thus, the conventional SELEX with the natural nucleic acid library may not be able to obtain the aptamers with the desired affinity in some cases.

A variety of nucleotide analogues have been introduced to enhance the affinity of aptamer and, accordingly, the success rate of SELEX.<sup>43–46</sup> Notably, a library of the 5-position-modified deoxyuridines was introduced to increase the aptamer's diversity and to create more hydrophobic interactions between targets and aptamer candidates.<sup>43–45</sup> In contrast to natural aptamers, contacts between target proteins and modified aptamers are mainly hydrophobic interactions instead of hydrogen-bonding or polar–polar interactions.<sup>44</sup> This minimizes the instability of the aptamer in different microenvironments that hold various pH values and salt concentrations, which may cause charge repulsion between the aptamer and target protein. As these nucleotide analogues can be recognized by commercially available polymerases,<sup>45</sup> they are compatible with the amplification step of the conventional SELEX. The modified single-stranded DNA library has been used to generate aptamers against protein targets where unmodified single-stranded DNA candidates have failed, with an overall success rate as high as 84% in a large-scale selection.<sup>43</sup> This type of aptamer is also known as SOMAmer (slow off-rate modified aptamer) and is now applied to cancer diagnostics<sup>47</sup> and biomarker discovery for diseases such as chronic kidney disease<sup>43</sup> and lung cancer.<sup>48</sup> Another similar approach that enhances base hydrophobicity and

improves the diversity of the aptamer library was reported by Kimoto *et al.*<sup>46</sup> A hydrophobic but artificial base (7-(2-thienyl)imidazo[4,5-*b*]pyridine) was added to the candidate sequences. The modified library was used to generate aptamers against VEGF<sub>165</sub> and interferon- $\gamma$ , and the resulted aptamers have extremely low dissociation constants ranging from low pico- to high femtomolar (fM), which are 100- to 5000-fold lower than that of unmodified aptamers. The examples above demonstrate that the affinity problem in aptamer design may be effectively resolved by increasing the diversity of nucleotide building blocks and decreasing charge repulsion. This approach may also significantly diversify the target range of aptamers, in general.

**Target Stimulation and Inhibition.** To date, there are more than 900 aptamers<sup>49</sup> generated from SELEX and developed for a broad spectrum of diagnostic and therapeutic applications. Although the aptamers in clinical trials are all able to inhibit their targets and show promising efficacy, these target-inhibiting (or stimulating) aptamers only account for a small portion of all reported aptamers. As mentioned earlier, high-affinity aptamers identified *via* SELEX may be able to bind well to the target, but they may not be able to act on the functional epitopes of the targets. As a result, post-SELEX screening is often performed to obtain an aptamer with this desired agonistic or antagonistic functionality.<sup>50,51</sup>

Instead of using the entire protein which contains both functional and nonfunctional epitopes, Jeon *et al.* used a conserved and functional epitope of influenza hemagglutinin as a target to ensure that the generated aptamer can block this particular epitope and accordingly show functionality.<sup>52</sup> Additionally, a competition-based selection approach called "epitope-specific SELEX" has been reported to generate antagonistic aptamers against the sialic acid receptor binding site of hemagglutinin.<sup>53</sup> The hemagglutinin-specific pool was first obtained and enriched through the conventional SELEX route. Aptamers against the desired domain were subsequently displaced from hemagglutinin by excess fetuin, an epitope competitor. Thus, the resulting aptamers are capable of blocking the epitope and show the antagonistic functionality of anti-hemagglutination, as well. Waybrant *et al.* used another approach to obtain epitope-specific aptamers by denaturing the desired domain of the target protein.<sup>54</sup> An aptamer against the chemokine domain of fractalkine (CX<sub>3</sub>CL1) protein was generated *via* this approach. First, the candidates that bind to either chemokine domain or another unstructured domain (mucin-like stalk) were generated through a conventional SELEX route. After that, the protein was denatured and incubated with the aptamer candidates. Only the candidates recognizing the unstructured domain were still interacting with the denatured fractalkine, so these were removed from the

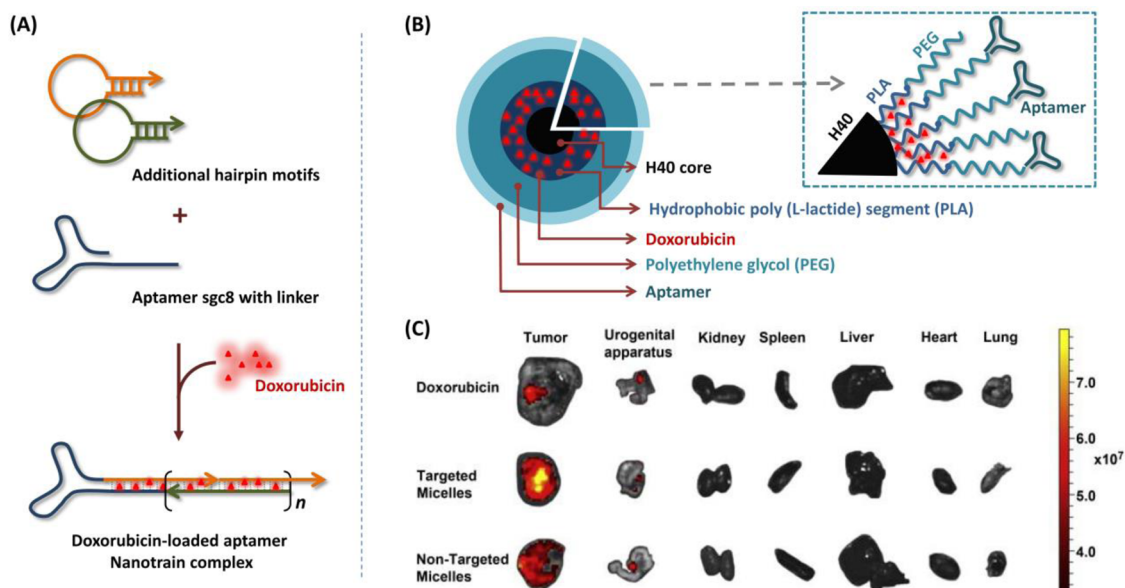


**Figure 3.** Upgrading aptamers with drugs through noncovalent interactions. (A) Aptamer nanotrain for leukemia therapeutics. Two hairpin motifs assemble a repeat unit of the nanotrain, and the aptamer is also coupled *via* nucleic acid hybridization. After assembly, doxorubicin intercalates the duplex region of the nanotrain. (B) Doxorubicin-loaded unimolecular micelle designed for prostate cancer therapy. This micelle comprises of a hyperbranched Boltorn H40 core with a PLA inner shell and a PEG outer shell. The doxorubicin is loaded in the inner shell *via* hydrophobic interaction, and the anti-PSMA aptamer (A10) is attached to the outer shell. (C) Enhancement in doxorubicin biodistribution by integrating the aptamer and micelle technologies. The accumulation of targeted micelles in the tumor (coupled with the aptamer A10) is significantly higher than that in other groups. Figure reproduced with permission from (A) ref 61 and (B,C) ref 68. Copyright 2013 Elsevier.

collected protein–candidate complexes and other chemokine-specific candidates accordingly remained in the supernatant. The resulting aptamer shows binding capability with the chemokine domain under the competition assay with epitope-specific antibody, and it may have functionality because it can block the interaction between this epitope and a receptor such as CX<sub>3</sub>CR1.

**Ligand–Payload Coupling.** The above-mentioned methods for the selection of a target-inhibiting (or stimulating) aptamer cannot be generalized as they are customized for an aptamer–target pair. For example, the functional epitopes may not be located at successive regions, rendering it difficult to artificially create a target epitope for the aptamer selection. Also, the competition and denaturation methods require some particular steps, which may not be adoptable in other cases. As a result, there is no selection technology that can guarantee the generation of this type of aptamer. Instead, an easier and more direct way to impart functionality to aptamers is to link them to a therapeutic payload *via* either covalent or noncovalent linkages.

**Aptamer–Drug Nanocomplexes.** Since the secondary structure of most aptamer backbones contains one or multiple duplex regions, some drugs<sup>55–58</sup> or dyes<sup>59</sup> can be noncovalently linked *via* intercalation. They can be loaded on the aptamer and released when the aptamer recognizes the target. Doxorubicin is a widely used therapeutic drug for this design of an aptamer–drug nanocomplex, which can specifically kill the

target-expressing cancer cells.<sup>55–57</sup> To improve the loading and drug efficacy, some additional duplexes<sup>60,61</sup> or origami<sup>62</sup> approaches were used. A “nanotrain” design was proposed to enhance the efficiency of doxorubicin loading.<sup>61</sup> A repeat unit of the nanotrain structure was assembled by annealing two hairpin DNA motifs and the aptamer against human protein tyrosine kinase-7 (sgc8)<sup>63,64</sup> *via* hybridization (Figure 3A). This aptamer–doxorubicin nanotrain can selectively recognize and inhibit the leukemia cell line, CCRF-CEM, which overexpresses the aptamer’s target protein. The efficacy of this aptamer–drug nanocomplex was validated in a xenograft mouse model with significantly reduced tumor growth and prolonged survival.<sup>61</sup>

Since aptamers incorporated with a wide range of functional groups are available from the manufacturer, direct covalent conjugation is another way to link an aptamer with the therapeutic drug. Several proof-of-concept studies have demonstrated *in vitro* that direct conjugation can improve the specificity of drugs, which originally hold no targeting ability.<sup>65–67</sup> However, this strategy may have some limitations: First, the drug may not have a functional group suitable for conjugation. Second, conjugation may affect the potency of the drug. Third, the release profile may need optimization. To address these issues, an aptamer-conjugated doxorubicin-loaded unimolecular micelle was developed.<sup>68</sup> This drug platform contained a hyper-branched aliphatic polyester core, a hydrophobic poly(lactic acid) (PLA) inner shell, a hydrophilic

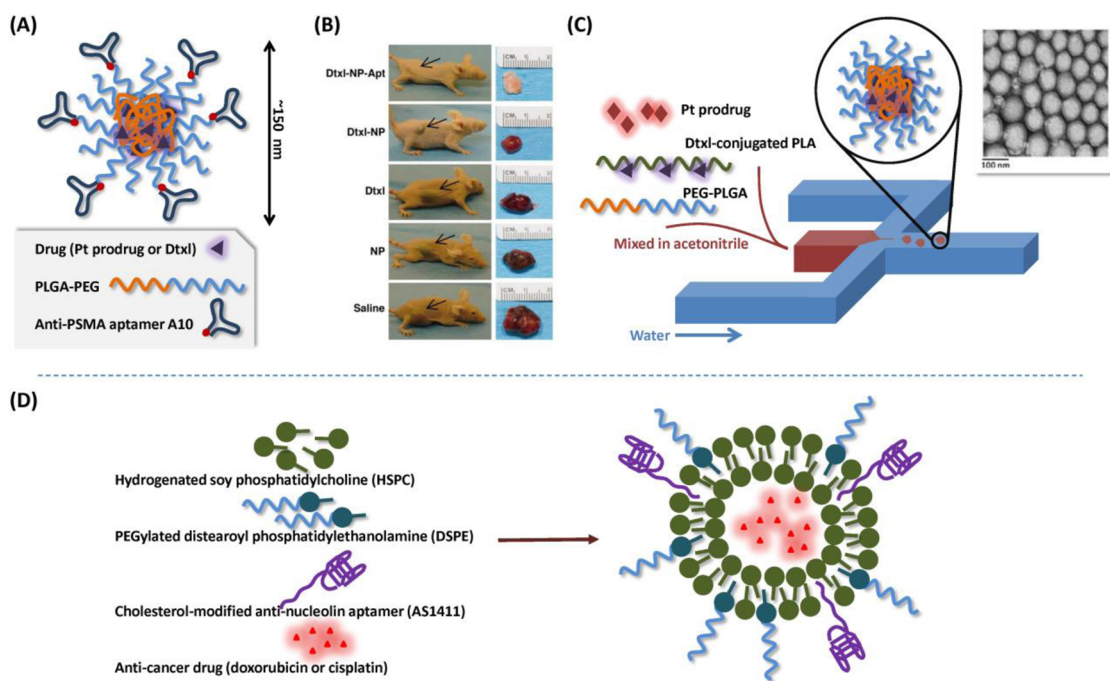


**Figure 4.** Polymeric and liposomal drug formulations coupled with aptamer technology for cancer therapeutics. (A) Schematic structure of aptamer-PEG-PLGA nanoparticle designed for chemotherapeutic drug delivery. The drug is encapsulated, and the nanoparticle is formed through nanoprecipitation. The aptamer A10 is conjugated onto the nanoparticle surface by EDC/NHS chemistry. (B) Comparison of the preclinical outcome of nanoparticle treatment. (C) Microfluidic technology for generation of monodispersed PEG-PLGA nanoparticles (inset: TEM image of nanoparticles generated from the microfluidic system). (D) Schematic of the aptamer-liposomal system for doxorubicin delivery. With a cholesterol modification, the antinucleolin aptamer AS1411 could be directly anchored with the nanoparticle during liposome formation. Figure reproduced with permission from (A,B) ref 70, copyright 2006 National Academy of Sciences; (C) ref 73 and (D) ref 80, copyright 2013 Royal Society of Chemistry.

polyethylene glycol (PEG) outer shell, and a surface conjugated with the aptamer-recognizing prostate-specific membrane antigen (PSMA), which is known as A10.<sup>69</sup> As shown in Figure 3B, the doxorubicin was loaded into the hydrophobic segment of the micelle. The drug-releasing mechanism is based on the hydrolysis of the polyester core, which is pH-sensitive. In an acidic microenvironment, the release rate of drug is nearly 2-fold higher than at neutral conditions, which means that this platform should be stable during the circulation and release the doxorubicin within the endosome or under an acidic tumor microenvironment. Furthermore, the anti-PSMA aptamer can enhance the efficacy of a doxorubicin-loaded micelle. This rationale is confirmed by *in vivo* distribution evaluation at 6 h post-administration (intravenous) when aptamer-conjugated doxorubicin micelles show 4-fold and 1.5-fold improvement compared with conventional doxorubicin and nontargeted doxorubicin micelles, respectively (Figure 3C).<sup>68</sup>

An aptamer-coupled PEG-poly(D,L-lactic-co-glycolic acid) (PLGA) nanoparticle was also developed for anti-cancer drug delivery and evaluated in the prostate cancer model (Figure 4A).<sup>70</sup> PLGA was first modified with PEG *via* 1-ethyl-3-(3-dimethylaminopropyl)-carbodiimide (EDC)/N-hydroxysuccinimide (NHS) chemistry, and the resultant PEG-PLGA docetaxel

nanoparticles were formed by nanoprecipitation. After conjugation of the anti-PSMA aptamer on the nanoparticle surface, the aptamer-drug complex showed significant efficacy in a murine prostate tumor model. Five of seven mice treated with aptamer-PEG-PLGA-docetaxel nanoparticles showed complete tumor regression, whereas only two and none of seven mice showed regression in the groups of nontargeted PEG-PLGA-docetaxel nanoparticles and docetaxel, respectively (Figure 4B).

The same group also used the same PEG-PLGA formulation to deliver cisplatin for prostate cancer treatment.<sup>71</sup> As cisplatin is practically insoluble in organic solvent, the authors encapsulated the hydrophobic platinum(IV) prodrug *via* nanoprecipitation. When the aptamer-PEG-PLGA-platinum(IV) complex was internalized, the platinum prodrug would be released after endosome escape and reduced to an active form, which can interact with the chromosome of the cancer cell. This approach increased not only encapsulation efficiency but also the potency of the platinum prodrug. Additionally, the preclinical evaluation factors such as maximum treatment dosage, biodistribution, and pharmacokinetics were also investigated.<sup>72</sup> Compared with cisplatin or the nontargeted platinum(IV) prodrug, this format was much safer and provided a longer half-life of active platinum.



In an LNCaP subcutaneous xenograft mouse model, an aptamer-coupled nanoparticle or cisplatin was intravenously administered twice every week. Mice treated with the nanoparticles showed an outcome (tumor regression) the same as those treated with cisplatin, but the required dosage of the nanoparticle formulation was only 1/3 of that of cisplatin. To improve the efficacy and to better control the formulation of the nanoparticle, co-delivery and the microfluidic production concepts were introduced (Figure 4C) to encapsulate both docetaxel and platinum(IV) prodrug in aptamer-coupled PEG–PLGA/PLA nanoparticles in a well-controlled environment.<sup>73</sup> The microfluidic technique precisely produced 100 nm nanoparticles with a small polydispersity index (<0.10).

A similar PLGA nanoparticle approach was used by Guo *et al.* to deliver paclitaxel for glioma treatment.<sup>74</sup> PEG–PLGA nanoparticles encapsulating paclitaxel were conjugated with antinucleolin aptamer, AS1411. This formulation showed much higher efficacy compared with the conventional paclitaxel drug (Taxol) *in vivo* and significantly increased survival rate and reduced tumor size. Overall, this aptamer-coupled PEG–PLGA drug delivery system has promising potential for translation because, first, both PLGA and PEG are well-studied biomaterials found in many FDA-approved formulations<sup>75,76</sup> and, second, the preclinical study of this nanocomplex format is comprehensively evaluated.<sup>72,74</sup>

Liposomal delivery platform is another significant formulation in the field of drug development, and many liposome-based drugs have been approved or are being evaluated in clinical trials.<sup>77,78</sup> Compared with other nanoparticle platforms, constructing an aptamer-coupled liposome may be easier since cholesterol-modified aptamers are commercially available, and liposomes can be directly anchored with a cholesterol-modified aptamer during nanoparticle formation (Figure 4D).<sup>79,80</sup> This advantage has been used to develop aptamer-coupled liposomes to specifically deliver cisplatin<sup>79</sup> and doxorubicin.<sup>80</sup> The antinucleolin aptamer, AS1411, for breast cancer cell targeting, coupled to this liposomal design, killed cancer cells with high specificity. This aptamer–doxorubicin liposome formulation inhibited breast tumor growth induced by estrogen as no significant growth of the tumor was observed in the group treated with the aptamer–doxorubicin liposome, while the size of the tumor in the control group increased 166%.<sup>80</sup> Besides the above-mentioned formulation, other types of aptamer-coupled nanoparticle systems for targeted drug delivery have also been reported.<sup>81–83</sup> Although these studies reported promising designs and impressive *in vitro* efficacies, *in vivo* validations are required for translation.

**Aptamer–Nucleic Acid Nanocomplexes.** In addition to small-molecule drugs, nucleic acid is another class of

therapeutic payload for targeted therapy. With respect to applications, nucleic acid payloads can be divided into two main types: nucleic acids for (1) gene silencing and (2) transfection. Small interfering RNA (siRNA), small hairpin RNA (shRNA), micro-RNA (miRNA), and antisense oligonucleotides are designed for knocking down a certain gene (deleting a gene function) to kill certain types of cells. In contrast, plasmid DNA or mRNA are used for transfection to deliver a certain gene (adding a gene function) to cure a disease. To date, most studies focus on the development of aptamer-mediated siRNA, shRNA, or miRNA delivery systems for gene silencing applications. This is an emerging class of gene therapy particularly promising for cancer therapy.

Similar to drug delivery, the easiest strategy for aptamer-based nucleic acid delivery is to link the therapeutic nucleic acid directly to the aptamer. This is known as an aptamer–therapeutic nucleic acid chimera (Figure 5A). Anti-PSMA RNA aptamer A10 was the first aptamer used for siRNA delivery, and the passenger strand of siRNA was directly synthesized with the aptamer.<sup>84</sup> Two siRNAs targeting the genes of polo-like kinase 1 (PLK1) and B-cell CLL/lymphoma 2 (BCL2), which are the common oncogenes engendered by most cancer cells, were applied, and these two aptamer–siRNA chimeras showed significant knock-down efficiency on the PSMA-overexpressing cell line, LNCaP. Furthermore, intratumoral treatment of aptamer–siRNA chimeras significantly inhibited tumor progression and reduced the size of the tumor in the case of the LNCaP cell-derived tumor-bearing mice, whereas no significant regression was observed in PC3-cell-derived tumor-bearing mice. In addition to the prostate cancer model, the aptamer–siRNA chimera was also tested in the non-small lung cancer model.<sup>85</sup> The aptamer AS1411 was linked to siRNA-targeting Snail family zinc finger 2 (SLUG) and neuropilin 1 (NRP1), both related to the tumor metastasis. As expected, the aptamer–siRNA chimera applied either individually (AS1411-SLUG or AS1411-NRP1) or synergistically (AS1411-SLUG plus AS1411-NRP1) showed significant tumor regression (Figure 5B). Furthermore, the synergistic treatment using two chimeras *via* intratumoral injection not only reduced the number of circulating tumor cells (Figure 5C) but also inhibited angiogenesis in the tumor.

The chimeras Chi-29b<sup>86</sup> and GL21.T-let<sup>87</sup> are additional examples of direct conjugation of the aptamer to a therapeutic nucleic acid. Chi-29b comprises an anti-mucin 1 (MUC1) aptamer<sup>88</sup> and miRNA miR-29b<sup>89</sup> for ovarian cancer treatment.<sup>86</sup> MUC1 protein is a common marker that is overexpressed in most cancer cells, including ovarian cancer cell lines, OVCAR-3 and OVAC420. The miRNA miR-29b interacts with the mRNAs of the DNA methyltransferase (DNMT) family, which regulate the DNA methylation.<sup>89</sup> This chimera was designed to specifically recognize the

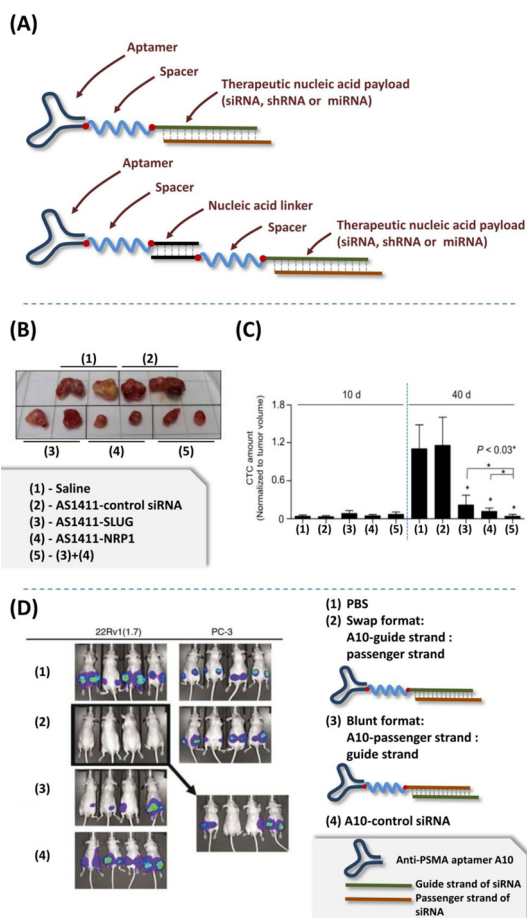


**Figure 5.** Aptamer nanomedicine in gene therapy for cancer treatment. (A) Two common strategies for linking aptamers with siRNAs. Direct synthesis approach (the upper case): aptamer is directly synthesized with a therapeutic nucleic acid payload (in this case, the payload is siRNA). Sticky end approach (the lower case): the chimera is formed by hybridizing the aptamer and the therapeutic nucleic acid (siRNA) *via* complementary sticky ends. (B) Preclinical outcome of the aptamer-siRNA chimera in the murine lung cancer model. Mice were intratumorally given with two aptamer-siRNA chimeras (AS1411-SLUG and AS1411-NRP1). Both single treatments (either AS1411-SLUG or AS1411-NRP1) and synergistic treatments (AS1411-SLUG and AS1411-NRP1) inhibit the tumor growth. (C) Number of circulating tumor cells after the treatment. The synergistic treatment of two aptamer-siRNA chimeras significantly reduces circulating tumor cells in the blood. (D) *In vivo* optimization of aptamer-siRNA chimera design. The 22Rv1 (PSMA-) and PC-3 (PSMA+) xenograft mice are intravenously administered with the aptamer-siRNA chimera (A10-PLK1). Compared with the blunt format (linking the passenger strand of siRNA with the aptamer), the swap format shows better *in vivo* specificity. Figure reproduced with permission from (B,C) ref 85, copyright 2014 Elsevier, and (D) ref 95, copyright 2009 Nature Publishing Group.

MUC1-overexpressed cancer cells and to inhibit the function of the DNMT family and accordingly rescue PTEN (phosphatase and tensin homologue) expression.<sup>86</sup> This approach inhibited the methylation of the PTEN promoter and up-regulated the PTEN expression in the OVCAR-3 ovarian cancer model both *in vitro*<sup>86</sup> and *in vivo*.<sup>90</sup> Moreover, this chimera was also potent against tumors derived from OVAC420 and

paclitaxel-resistant OVCAR-3 cells. Interestingly, this chimera killed the above-mentioned cancer cells through different pathways distinct from that of wild-type OVCAR-3. For OVAC420, rather than reversing of the PTEN expression, the chimera showed potency by inhibiting the mitogen-activated protein kinase (MAPK) pathway and insulin-like growth factor 1 (IGF1) expression. In the case of paclitaxel-resistant OVCAR-3, it was presumed that the chimera reduced the growth rate of tumor *via* three routes: (1) up-regulation of PTEN (induction of apoptosis), (2) inhibition of the MAPK/IGF1 pathway, and (3) inhibition of aldehyde dehydrogenase 1 expression.<sup>90</sup> Similarly, GL21.T-let is also an aptamer-miRNA chimera,<sup>87</sup> which is composed of an antagonistic aptamer against the Axl receptor tyrosine kinase<sup>91</sup> and the human miRNA let-7g.<sup>92</sup> This study demonstrates that direct conjugation of aptamer and therapeutic nucleic acid does not influence the aptamer's affinity if the linkage between the aptamer and the payload is optimized ( $K_D$  of GL21.T-let and its parent aptamer: 19 vs 12 nM).<sup>87,91</sup> Moreover, a synergistic effect from the aptamer and the miRNA has been demonstrated in this study.<sup>87</sup> The chimera GL21.T-let showed more than 20% improvement on *in vitro* inhibition of cancer cell growth and migration and improved the outcome in the *in vivo* assessment. With the assistance of the aptamer, the chimera specifically reduced the volume of the Axl-expressing tumor rather than that of the Axl-negative tumor. However, the transfection efficiency of GL21.T-let is more than 10 times lower than that of the conventional transfection agent, which indicates the necessity of a nanoparticle delivery system for effective transfection.

The aptamer-therapeutic nucleic acid chimera can also be used to improve the efficacy of ionizing radiation for prostate cancer treatment.<sup>93</sup> The aptamer A10 has been linked with the shRNA against DNA-activated protein kinase (DNAPK) related to the pathway of DNA repair. This chimera can localize at the tumor site and inhibit the DNA repair after the treatment with ionizing radiation and effectively serves as a radio-sensitization agent. Combined with the radiation treatment, the intratumoral treatment with the A10-DNAPK shRNA chimera significantly inhibited tumor progression compared with nontargeted DNAPK shRNA.

This design also inspired interests in the structural study of the chimera, where the secondary structure of aptamer-shRNA chimera was systematically investigated by its correlation with *in vitro* gene silencing.<sup>94</sup> In addition, an *in vivo* optimization of siRNA has also been reported.<sup>95</sup> In this study, the aptamer-siRNA chimera (A10-PLK1)<sup>84</sup> was further optimized for systemic administration by tuning the secondary structure and swapping guide/passenger strands of the siRNA, leading to improved potency.<sup>95</sup> This study is the first to show significant regression of tumors by intraperitoneal treatment (Figure 5D).

Besides the aptamer–therapeutic nucleic acid chimera, aptamer–PEG–PLGA<sup>96</sup> and aptamer–PEG–liposome<sup>97</sup> nanoparticles have also been used to deliver nucleic acids for the treatment of prostate cancer. In the PEG–PLGA system (A10-Nano-ARHP8),<sup>96</sup> the aptamer A10 and plasmid-encoding shRNA (ARHP8) served as the ligand for PSMA targeting and the payload for silencing the expression of androgen receptor, respectively. Compared with the control group, the A10-Nano-ARHP8 nanoparticle intravenously administered prevented tumor growth in three different tumor models established by LNCaP, 22RV1, and LAPAC-4 prostate cancer cells. Compared with nontargeted nanoparticle, aptamer conjugation enhanced the local concentration of the payload ARHP8 in the tumor site (more than 2-fold higher than the nontargeted nanoparticle) and resulted in better knockdown efficiency (~90%) of the androgen receptor at the mRNA level. On the other hand, a PEGylated cationic liposomal system has been also recently used for aptamer-based siRNA delivery.<sup>97</sup> A siRNA designed for malignant melanoma treatment was encapsulated in the liposome, and its surface was decorated with the aptamer AS1411 *via* a thiol–maleimide reaction. Although this system shows accumulation in the tumor site superior to that of the nontargeted liposome and free siRNA, its knockdown efficiency (45%)<sup>97</sup> is not as high as the above-mentioned PEG–PLGA system.<sup>96</sup> This may be due to the undesired interaction between its cationic surface and aptamer backbone, which will be discussed in the latter section of this review.

**Aptamer Nanomedicine for In Vivo Diagnostics.** Upgrading an aptamer for *in vivo* diagnostics is also important because early diagnosis may be the most important step in cancer therapy. Aptamer nanomedicine has been applied in optical, magnetic resonance, and nuclear medicine imaging. For optical imaging, the aptamer is typically labeled with a fluorescent tag. The aptamer TD05<sup>98</sup> which recognizes the Burkitt's lymphoma cell line, Ramos, shows the capability of distinguishing the tumor site from other tissues *in vivo*.<sup>99</sup> Cy5-labeled TD05 specifically accumulated in the tumor site of Ramos-bearing mouse with a signal-to-background (S/B) ratio as high as 115.<sup>100</sup> This aptamer–dye complex format was also used for *in vivo* visualization of lung and liver tumors.<sup>101</sup> However, the use of an aptamer–dye complex is an “always on” detection method, which emits fluorescence before target recognition. It results in high levels of background signal and reduces sensitivity. To address this problem, a design derived from aptamer beacons, which have been widely used for *in vitro* sensing,<sup>102–104</sup> was proposed.<sup>105</sup> This beacon only fluoresces when it interacts with the target. The structure of this aptamer–dye complex is a hairpin construct, and the fluorescent readout is triggered by aptamer–target interaction (Figure 6A). When interacting with the target, the dye

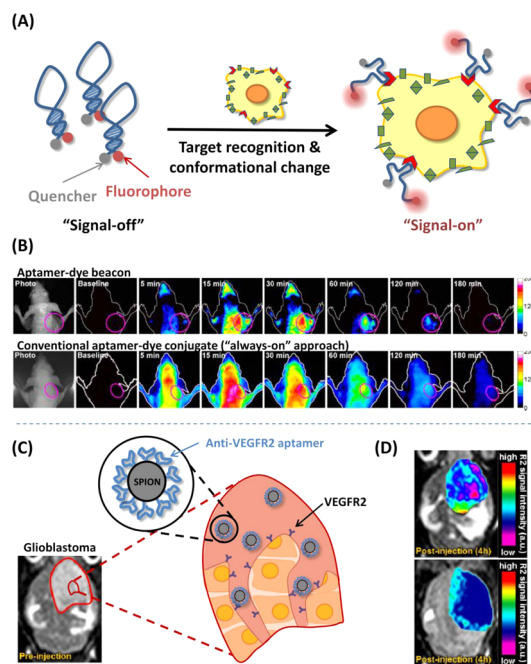


**Figure 6.** Aptamer nanomedicine for *in vivo* cancer diagnostics. (A) Aptamer–dye beacon design for cancer imaging. The hairpin beacon is constructed by an aptamer and the assistance strand. Once the aptamer moiety interacts with the target, the fluorophore departs from the quencher and accordingly emits the fluorescence due to the conformational change of the aptamer. (B) Comparison of *in vivo* specificity between the aptamer–dye beacon and the conventional “always on” aptamer–dye conjugate. The beacon design significantly improves the signal-to-background ratio and shows better specificity. (C) Scheme of aptamer-coupled SPION nanocomplex for glioblastoma imaging. Since the aptamer targets VEGF receptor 2 (VEGFR2), which is an angiogenic marker, the application of an aptamer–SPION nanocomplex facilitates visualization of angiogenic vasculature of the tumor. (D) Signal enhancement of the aptamer–SPION nanocomplex. The aptamer improves the localization of SPION in the tumor site and results in a better magnetic resonance imaging signal. Figure reproduced with permission from (A,B) ref 105 and (C,D) ref 108. Copyright 2013 Springer.

is separated from its complementary quencher due to the conformational change of the beacon and results in fluorescence emission. Compared with the “always on” design, the beacon construct significantly enhances the S/B ratio (Figure 6B).

Sensitivity enhancement is also important for magnetic resonance imaging (MRI). Aptamer-coupled MRI contrast agents improve sensitivity by providing enhanced resolution of tumor tissue. Paramagnetic and superparamagnetic agents are two major materials that improve the longitudinal and transverse relaxations to enhance contrast, respectively.<sup>106</sup> A manganese ( $Mn^{2+}$ ) nanoparticle is one of the paramagnetic materials widely used for MRI and is less toxic than the chelate form. A silica-coated  $Mn_3O_4$  nanoparticle was recently coupled with the antinucleolin aptamer AS1411 for *in vivo* tumor imaging.<sup>107</sup> This aptamer-coupled nanoparticle enhanced sensitivity by 2-fold after a 12 h treatment and did not cause significant

inflammation and toxicity when analyzed histologically and biochemically 10 days after treatment. In addition, superparamagnetic iron oxide nanoparticles (SPION) are also used with an aptamer as a targeted imaging agent for tumor visualization in MRI.<sup>108</sup> An aptamer-coupled SPION system for glioblastoma diagnosis was reported recently, where a DNA aptamer against VEGF receptor 2 was used to target the angiogenic vessels surrounding the tumor (Figure 6C). Notably, this aptamer–SPION can cross the brain–blood barrier and enhance the MRI signal by 25%, which is also significant compared with the nontargeted SPION (Figure 6D).

Aptamer-based nuclear medicine imaging agents are developed before optical imaging and MRI. The aptamer recognizing neutrophil elastase was the first aptamer linked with technetium (<sup>99m</sup>Tc) for *in vivo* diagnosis of inflammation disease.<sup>109</sup> In a mice model, where the aptamer–<sup>99m</sup>Tc complex was compared with the conventional antibody-based imaging agent, the aptamer–<sup>99m</sup>Tc complex achieved a maximum signal in 2 h with a S/B ratio of  $4.3 \pm 0.6$ , whereas the antibody system needed 3 h and provided worse contrast (S/B ratio =  $3.1 \pm 0.1$ ). In a subsequent study, an RNA aptamer against tenascin-C,<sup>110</sup> an extracellular matrix protein expressed under tumor growth, was modified with a <sup>99m</sup>Tc chelate and applied in the same model for tumor imaging.<sup>15</sup> Consistently, the aptamer–<sup>99m</sup>Tc complex showed higher S/B ratio (180 vs 5) and shorter accumulation time (16 vs 40 h) compared with the antibody system. The aptamer–<sup>99m</sup>Tc complex system was also optimized *in vivo* by tuning the chelate complex and ligand-per-chelate number to improve the sensitivity and reduce accompanied toxicity.<sup>111</sup>

**Aptamer Co-delivery Nanocomplexes.** Different approaches for designing aptamer nanocomplexes have been highlighted in previous sections. An aptamer-based co-delivery system can be easily constructed by combining two or more of these approaches. This may be the ultimate goal for therapeutics, diagnostics, or even theranostics, that is, “efficacy by design”. For example, combining therapeutic and diagnostic payloads allows aptamer nanocomplexes to detect and kill tumor cells simultaneously. Alternatively, by multiplexing two different drugs or therapeutic nucleic acids (or a combination of both), we may be able to tackle more complex therapeutic problems such as the drug resistance of cancer cells.

For theranostics application, a quantum dot–aptamer–doxorubicin nanocomplex was proposed.<sup>112</sup> The doxorubicin was loaded onto the backbone of the anti-PSMA aptamer A10 through intercalation that was previously discussed. The 5′-end of the aptamer was modified with an amine group, which was used for conjugation with the quantum dot *via* EDC/NHS chemistry. When the nanocomplex was constructed, the fluorescence of the nanocomplex would be “turned

off” due to the fluorescence resonance energy transfer (FRET). The fluorescence of quantum dot was quenched by doxorubicin, and that of doxorubicin was quenched by interacting with the aptamer. When interacting with the target (PSMA+) cell, the doxorubicin was released due to the conformational change, and the FRET effect was accordingly eliminated, which resulted in the emission of quantum dot. Therefore, this strategy can both identify and kill cancer cells simultaneously.

This idea was extended to *in vivo* theranostics with some minor modification by using the anti-MUC1 aptamer combined with epirubicin and SPION as the drug and imaging agent, respectively.<sup>113</sup> Similar to doxorubicin, epirubicin has a fluorescence property that could be quenched by interaction with the aptamer. In an *in vivo* colon cancer cell xenograft model, intravenous administration of this nanocomplex system significantly inhibited tumor growth compared with the treatment with nontargeted epirubicin. However, unlike the quantum dot system, the SPION is also an “always on” approach, which has the problem of low S/B ratio, which needs to be addressed before translation.

In contrast to intercalation, the two-step direct conjugation is another option to link both the aptamer and therapeutic drug. Savla *et al.* conjugated a quantum dot with the anti-MUC1 aptamer and doxorubicin through EDC/NHS and hydrazine chemistry, respectively.<sup>114</sup> Because the hydrazine bond is unstable under acidic conditions, more than 35% of doxorubicin was released from the conjugate after 5 h at pH 5. Hence, we can expect this aptamer–quantum dot–doxorubicin conjugate to be stable in physiological environment, and the chemotherapy drug would be released after it is internalized through receptor-mediated endocytosis. The *in vivo* evidence showed that this conjugate highly accumulated in the tumor site but not in other organs compared with an unmodified quantum dot.

## APTAMER NANOMEDICINE AT THE APPLICATION STAGE

If the issues at the design stage are resolved, aptamer nanomedicine may have a higher chance for clinical translation. However, several *in vivo* barriers remain. First, as most aptamers are obtained from *in vitro* selection under a simplified environment, they may lose specificity when applied *in vivo* when the environment becomes more complex. Second, aptamers may have poor pharmacokinetics and biodistribution due to problems related to immunogenicity, nuclease degradation, and physical characteristics. For instance, an aptamer nanomedicine agent may be cleared/degraded before reaching the tumor site, or its polar nature may prevent it from sufficiently penetrating the tumor. In this section, we will discuss

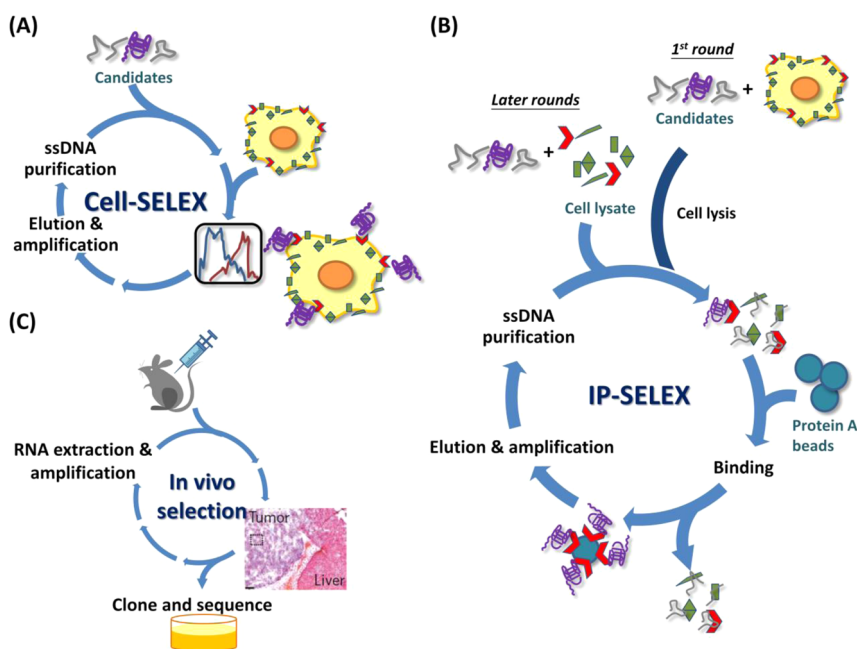


**Figure 7.** Strategies to improve *in vivo* specificity and reduce off-target effects of aptamer therapeutics. (A) Cell-SELEX to generate the aptamer recognizing a target cell. Instead of a protein, a cell is used as the target during the entire SELEX process. (B) IP-SELEX as a combinational approach for high-specificity aptamer generation. In IP-SELEX, immunoprecipitation is coupled with cell-SELEX. The cell-specific candidates are obtained through a first round of cell-based selection, and the protein-specific aptamers are subsequently generated through immunoprecipitation. This can ensure that the generated aptamers will bind to the desired target and have high specificity. (C) *In vivo* selection for tissue-specific aptamer generation. The tumor-bearing mouse is intravenously administered with the candidate pool, and the tissue-bound candidates are collected and then amplified for the next round. Thus, the aptamer selected has a high specificity for recognizing the tumor tissue. Figure reproduced with permission from (A) ref 116, copyright 2010 Nature Publishing Group; (B) ref 50, copyright 2009 Federation of American Societies for Experimental Biology; and (C) ref 118, copyright 2010 Nature Publishing Group.

barriers affecting the success of aptamer nanomedicine for *in vivo* application and highlight significant work in this area.

***In Vivo* Specificity.** Aptamers with excellent *in vitro* affinity have been used for diagnostic applications.<sup>43,115</sup> However, they still face *in vivo* off-target problems because conventional SELEX is only based on the interaction between pure protein and nucleic acid candidates, which oversimplifies the actual *in vivo* environment. To address this problem, instead of using pure protein, cell-SELEX was proposed using cells as targets to mimic the *in vivo* environment to generate cell-specific aptamers (Figure 7A),<sup>116</sup> which can distinguish different cells not only *in vitro* but also *in vivo*.<sup>63,105</sup> However, this cell-SELEX method needs an additional postselection identification to verify what the complementary target is. In this combined cell-SELEX and immunoprecipitation (IP) method known as IP-SELEX,<sup>50,117</sup> the aptamer library is first incubated with a target-overexpressing cell line during the first round of SELEX. In subsequent selection rounds, candidates are incubated with target proteins that are immunoprecipitated from the cell surface (Figure 7B). This method ensures that the aptamer recognizes the desired protein target without losing cell specificity. Mi *et al.* further demonstrated the possibility of *in vivo* selection of the aptamer

(Figure 7C).<sup>118</sup> In this study, the RNA library was first intravenously injected into tumor-bearing (intrahepatic colorectal metastases) mice. RNA candidates isolated from the tissue of the hepatic tumor were then collected and amplified. After 14 rounds of selection, sequences converged to three families, with aptamer 14–16 showing the highest affinity to the extracted tumor proteins. The target protein of aptamer 14–16 was also identified to be p68 helicase, an overexpressed oncoprotein of colon cancer. The specific recognition of p68 was further confirmed by inhibition assay and immunostaining. This *in vivo* selection method has also been used to discover another RNA aptamer that can cross the blood–brain barrier.<sup>119</sup> In this study, an RNA library with a random region composed of 40 nucleotides was administered into the mice through tail vein injection. After brain tissues were harvested from treated mice, aptamer A15 was found in the parenchymal fraction of the brain. Based on the results of *in vitro* internalization assays, it was speculated that aptamer A15 bound to the brain's endothelial cells and then penetrated into the blood-vessel-depleted parenchyma.

**Immunogenicity and Nuclease Degradation.** For aptamer therapeutics, immunogenicity and nuclease degradation may not be a serious impediment. Direct evidence showing immunogenicity of the aptamer has not been reported. For instance, no significant immunogenicity

is found in the monkey model where the anti-VEGF aptamer (pegaptanib) is administered at a dose that is 1000-fold higher than the therapeutic dose.<sup>120</sup> Similarly, the antinucleolin aptamer AS1411 is not immunogenic in the preclinical models of rats and dogs.<sup>121</sup>

Nevertheless, aptamers as nucleic acids may still be detected by Toll-like receptors (TLRs) 3, 7, 8, and 9, which stimulate the innate immune signaling pathways.<sup>122</sup> Fortunately, this may not be a significant issue for the aptamer therapeutics because aptamers can be synthesized using 2'-*O*-methylribonucleotides. Both *in vitro* and *in vivo* studies have shown that substitution of the guanine with 2'-*O*-methyl (2'-OMe)-guanine can significantly prevent the TLR-induced signaling pathway.<sup>123,124</sup> This substitution has also been widely used in siRNA studies to prevent immune stimulation.<sup>125,126</sup> For this reason, aptamers in clinical trials, such as pegaptanib, E10030, ARC1779, and BAX499, including the antidote pair (REG007), are incorporated with 2'-OMe modifications.<sup>16,24,27,29,34</sup>

The introduction of 2'-OMe modification prevents not only interaction with TLRs but also nuclease degradation. An *ex vivo* demonstration shows that the half-life of an unmodified aptamer is very short, and the functionality of the aptamer is totally neutralized after 10 min in plasma.<sup>127</sup> This implies that an unmodified aptamer is highly unstable in blood. Modifying some parts of the original sequence of the nucleic acid with 2'-OMe groups significantly prevents the aptamer from nuclease degradation.<sup>125,128</sup> For example, when all the nucleotides of the aptamer are modified with 2'-OMe groups, the *in vitro* half-life of the aptamer with the rat plasma is as long as 96 h.<sup>129</sup> Introducing 2'-fluoro modification confers similar protection against nuclease degradation.<sup>125</sup> The aptamers in clinical trials, such as pegaptanib, RB006 (the aptamer part of REG1), and ARC1905, are incorporated with 2'-fluoro ribonucleotides.<sup>16,25,27</sup> However, these modifications may reduce the aptamer's binding affinity.<sup>130</sup> Also, substitution positions of the aptamer sequence may require further optimization due to a lack of a prediction model regarding the relationship between the aptamer tertiary structure and sequence modification.

Capping with the inverted nucleotides is also a common strategy to reduce nuclease degradation by preventing the recognition by exonucleases. Ortigao *et al.* showed that capped oligonucleotide was stable after a 90 min incubation with serum, whereas the uncapped oligonucleotide degraded and lost its function after 30 min in serum.<sup>131</sup> This modification is often carried out in the aptamers, as well. For example, the aptamers pegaptanib, E10030, ARC1779, and ARC1905 are additionally capped with the inverted dT at the 3'-end.<sup>16,24,25,29</sup> The Spiegelmer mentioned previously is another approach. Due to the aptamer's chirality, it can be recognized neither by TLRs nor by nucleases, which recognize only D-form nucleic acids. Therefore, it

is less immunogenic and holds a longer half-life compared with other D-form aptamers or therapeutic nucleic acids.<sup>37</sup>

**Systemic Circulation.** Although the 2'-OMe modifications and capping with inverted nucleotides provide excellent protection against nucleases, the modified aptamers themselves are still rapidly cleared through renal filtration due to low molecular weight. Polyethylene glycol is commonly used to increase the molecular weight of the functional aptamer to prevent it from excretion *via* renal filtration. Healy *et al.* investigated the influence of PEGylation on the pharmacokinetics of the aptamer.<sup>129</sup> PEGylation leads to approximately 10-fold improvement in mean residence time (MRT), from 1.7 to 16 h with a 40 kDa PEG. Also, both MRT and elimination half-life are proportional to the molecular weight of PEG. Moreover, the administration route does not affect the elimination half-life in a monkey preclinical model.<sup>132</sup>

Conjugating the aptamer with a therapeutic payload may also change the circulation profile. Particularly, for nanoparticles (*e.g.*, quantum dots and PLGA nanoparticles), the size, charge, and hydrophobicity will lead to different biodistribution. The conjugation of the aptamer to therapeutic payloads may also make them more immunogenic due to an increase in molecular weight. Consequently, the biodistribution of the conjugated aptamer may be very different from that of the unconjugated aptamer.

In general, the reticuloendothelial system, also known as the monocyte–macrophage cell system, takes up the PEGylated aptamers and aptamer nanocomplexes. Hence, the liver, spleen, and lymph nodes are the major uptake organs of the conjugated aptamers.<sup>129,132</sup> In particular, the liver, which contains the Kupffer cells, is central in the clearance of the PEGylated aptamers or aptamer nanocomplexes. Nevertheless, the biodistribution of aptamer conjugates will vary with their actual size, charge, and the other physical characteristics. For example, in the aptamer–PLGA nanoparticle system for the drug delivery, an increase in surface density of the aptamer can enhance the rate of liver accumulation. Nanoparticles with 10% surface density of aptamer boosted liver accumulation from  $26.1 \pm 7.9\%$  (nonconjugated nanoparticle) to  $73.0 \pm 3.89\%$  of the injected nanoparticles.<sup>133</sup>

**Tumor Penetration.** Due to the rapid proliferation, the vessel architecture in the tumor is usually disorganized, and a population of cancer cells is in a hypoxia microenvironment with poor blood support. Also, the lack of functional lymphatics leads to a high interstitial fluid pressure in the microenvironment. These cause poor conventions and exacerbate the efficiency of drug delivery.<sup>134</sup> In addition, extracellular matrixes and stromal cells surrounding cancer cells may interfere with the drug targeting and slow the transport.

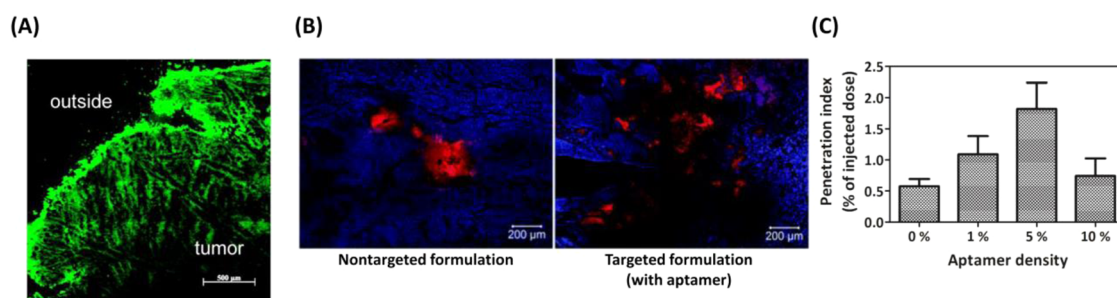


**Figure 8.** Enhancement of tumor penetration with aptamer technology. (A) Penetration barriers in cancer drug delivery. Due to the heterogeneous microenvironment and leaky vessel, the cancer drug has to travel through a long distance to target and kill cancer cells. (B) Enhanced penetration with the aptamer-coupled liposomal doxorubicin in *ex vivo* model. (C) *In vivo* optimization of aptamer density on the surface of PEG–PLGA nanoparticles. Figure reproduced with permission from (A) ref 135, copyright 2013 American Chemical Society; (B) ref 80, copyright 2013 Royal Society of Chemistry; and (C) ref 133, copyright 2008 National Academy of Sciences.

Consequently, the aptamer-coupled drug complex has to overcome these barriers before interacting with the cancer cells (Figure 8A).<sup>135</sup>

Recent studies demonstrate that the aptamer-coupled drug complex may be able to cross these barriers and penetrate into the tumor site more evenly. Xing *et al.* used an *ex vivo* model to compare the penetration efficiency of aptamer-coupled and nontargeted liposomal drugs.<sup>80</sup> The tumors were excised from the xenografts of mice and cultured with these drugs for 24 h to evaluate penetration. The presence of aptamer significantly improves the penetration over that of the nontargeted liposomes, which relies only on passive transport (Figure 8B). This may be expected because a study, comparing aptamer, nonspecific ligand, and antibody, has already revealed that aptamers have superior tumor uptake kinetics and longer tumor retention,<sup>15</sup> which may benefit aptamer nanocomplexes in tumor penetration. However, tumor penetration is influenced by cancer types, and there are currently no generalized approaches that can minimize the variations between different cancer models. Different cancer types will need different drug characteristics (*e.g.*, size, charge, shape, and molecular weight) to overcome the transport barrier.<sup>135,136</sup> Gu *et al.* optimized the surface aptamer density on the PLGA nanoparticles and evaluated its influence on drug penetration.<sup>133</sup> After intravenous administration of naked PLGA nanoparticles, only  $0.576 \pm 0.116\%$  of the treated dose (in weight ratio) penetrated into the tumor site. On the other hand, with a 5% surface density of aptamer on the PLGA nanoparticles, a 3-fold enhancement of drug penetration was observed (Figure 8C). Although it is a significant improvement, the penetration efficiency is still low and the results highlight the difficulty of tumor penetration even with the use of an efficient aptamer. Further innovations, perhaps through enzymatic, thermal, or ultrasonic measures to lower the transport resistance of the necrotic tumor region, would be required to improve the tumor penetration of aptamer cancer nanomedicine.

## PERSPECTIVE AND FUTURE DIRECTION

Cancer therapy against solid and metastasized tumors, in particular, remains ineffective. Aptamer nanomedicine is an emerging and promising class of therapeutics to address the challenges faced by current cancer therapy. Properties such as affinity, function, specificity, immunogenicity, pharmacokinetics, and penetration efficiency can be finely engineered to maximize the efficacy at the design and the application stages. Although some aptamer nanomedicines show great potential either in clinical trials or in the preclinical pipeline, this field is still in its infancy. Many obstacles mentioned in this review still need to be addressed. As current technology cannot ensure the generation of functional aptamers, functionalization with therapeutic payloads is still necessary for most cases. Hence design parameters such as the charge of payload (or drug carrier), length between aptamer and payload, and aptamer density, all of which are critical to generate functional aptamer–drug conjugates, have to be carefully optimized. For example, charged payloads may nonspecifically interact with the aptamer, and therefore, a spacer (*e.g.*, PEG or oligo(dT)) with a suitable length is necessary to reduce the interference and accordingly avoid the structural instability of aptamer.<sup>133,137</sup> The length of the spacer may also affect the aptamer folding, *in vivo* biodistribution, or interaction with the receptor target. In the case of the aptamer–nanoparticle platform, the surface density of the aptamer on the nanoparticle will be an additional factor. On one hand, a high ligand density enhances the cooperative binding avidity<sup>137</sup> and improves drug accumulation in the target tissue.<sup>133</sup> On the other hand, when the aptamer density on the nanoparticle is too high, there will be aptamer self-interaction and may lead to a deterioration in overall affinity.

In cancer therapy, a single drug is often not as efficacious as combinational drugs acting through multiple mechanisms.<sup>73,85,113,114</sup> Aptamer nanomedicine is highly compatible with combinational drug therapy.

However, the approach would require a better understanding of carrier design, drug-loading efficiency, and drug-releasing mechanism.<sup>138</sup> Another fruitful direction would be to apply aptamer nanomedicine toward cancer immunotherapy. Two studies have demonstrated this possibility by using an antagonistic aptamer recognizing CTLA4, a T cell receptor that negatively regulates the antitumor immunity of the T cell. This aptamer can serve as an adjuvant and improve the *in vivo* outcome by directly blocking the function of CTLA4 receptors<sup>139</sup> or silencing the tumor-promoting interactions on T cells when coupled with an siRNA.<sup>140</sup>

In summary, aptamer nanomedicine may address limitations of other ligands for targeted therapy in oncology. Aptamers have significant translation potential because they can be engineered as a safe, well-controlled, and robust delivery system.<sup>141</sup> Although barriers associated with design and *in vivo* application still exist, proof-of-concepts discussed in this review suggest that these barriers are surmountable. We may be able to find a more practical path toward clinical translation of aptamer nanomedicine by engineering aptamer nanomedicine with these barriers in mind.

**Conflict of Interest:** The authors declare no competing financial interest.

**Acknowledgment.** The authors would like to thank the kind input and useful comments from Dr. Pei-Lun Tsai at the University of Nottingham. Y.H.L. acknowledges fellowship support from the Ministry of Education (Taiwan). This work is supported by the Department of Defense (W81XWH-12-1-0261), NIH (RO1 AI096305, BRP HL109442), and the Grant-In-Aid of Research Program from Sigma Xi Research Society (G20131015280632).

## REFERENCES AND NOTES

- Nimjee, S. M.; Rusconi, C. P.; Sullenger, B. A. Aptamers: An Emerging Class of Therapeutics. *Annu. Rev. Med.* **2005**, *56*, 555–583.
- Bunka, D. H. J.; Stockley, P. G. Aptamers Come of Age—At Last. *Nat. Rev. Microbiol.* **2006**, *4*, 588–596.
- Stoltenburg, R.; Reinemann, C.; Strehlitz, B. SELEX—A (R)Evolutionary Method To Generate High-Affinity Nucleic Acid Ligands. *Biomol. Eng.* **2007**, *24*, 381–403.
- Tuerk, C.; Gold, L. Systematic Evolution of Ligands by Exponential Enrichment—RNA Ligands to Bacteriophage-T4 DNA-Polymerase. *Science* **1990**, *249*, 505–510.
- Ellington, A. D.; Szostak, J. W. *In Vitro* Selection of RNA Molecules That Bind Specific Ligands. *Nature* **1990**, *346*, 818–822.
- Sefah, K.; Phillips, J. A.; Xiong, X. L.; Meng, L.; Van Simaey, D.; Chen, H.; Martin, J.; Tan, W. H. Nucleic Acid Aptamers for Biosensors and Bio-analytical Applications. *Analyst* **2009**, *134*, 1765–1775.
- Mairal, T.; Ozalp, V. C.; Sanchez, P. L.; Mir, M.; Katakis, I.; O'Sullivan, C. K. Aptamers: Molecular Tools for Analytical Applications. *Anal. Bioanal. Chem.* **2008**, *390*, 989–1007.
- Tombelli, S.; Minunni, A.; Mascini, A. Analytical Applications of Aptamers. *Biosens. Bioelectron.* **2005**, *20*, 2424–2434.
- Shum, K.-T.; Zhou, J.; Rossi, J. J. Aptamer-Based Therapeutics: New Approaches To Combat Human Viral Diseases. *Pharmaceuticals* **2013**, *6*, 1507–1542.
- Zhou, J.; Bobbin, M. L.; Burnett, J. C.; Rossi, J. J. Current Progress of RNA Aptamer-Based Therapeutics. *Front. Genet.* **2012**, *3*, 234.
- Bunka, D. H. J.; Platonova, O.; Stockley, P. G. Development of Aptamer Therapeutics. *Curr. Opin. Pharmacol.* **2010**, *10*, 557–562.
- Fridman, W. H.; Teillaud, J. L.; Bouchard, C.; Teillaud, C.; Astier, A.; Tartour, E.; Galon, J.; Mathiot, C.; Sautes, C. Soluble Fc- $\gamma$  Receptors. *J. Leukocyte Biol.* **1993**, *54*, 504–512.
- Daeron, M. Fc Receptor Biology. *Annu. Rev. Immunol.* **1997**, *15*, 203–234.
- Nimmerjahn, F.; Ravetch, J. V. Fc-Receptors as Regulators of Immunity. In *Advances in Immunology*; Frederick, W. A., Ed.; Academic Press: New York, 2007; Vol. 96, pp 179–204.
- Hicke, B. J.; Stephens, A. W.; Gould, T.; Chang, Y. F.; Lynott, C. K.; Heil, J.; Borkowski, S.; Hilger, C. S.; Cook, G.; Warren, S.; et al. Tumor Targeting by an Aptamer. *J. Nucl. Med.* **2006**, *47*, 668–678.
- Ng, E. W. M.; Shima, D. T.; Calias, P.; Cunningham, E. T.; Guyer, D. R.; Adamis, A. P. Pegaptanib, a Targeted Anti-VEGF Aptamer for Ocular Vascular Disease. *Nat. Rev. Drug Discovery* **2006**, *5*, 123–132.
- Jager, R. D.; Mieler, W. F.; Miller, J. W. Medical Progress: Age-Related Macular Degeneration. *N. Engl. J. Med.* **2008**, *358*, 2606–2617.
- Ferrara, N.; Gerber, H. P.; LeCouter, J. The Biology of VEGF and Its Receptors. *Nat. Med.* **2003**, *9*, 669–676.
- Ferrara, N.; Damico, L.; Shams, N.; Lowman, H.; Kim, R. Development of Ranibizumab, an Anti-vascular Endothelial Growth Factor Antigen Binding Fragment, as Therapy for Neovascular Age-Related Macular Degeneration. *Retina* **2006**, *26*, 859–870.
- Friberg, T. R.; Tolentino, M.; Grp, L. S. Pegaptanib Sodium as Maintenance Therapy in Neovascular Age-Related Macular Degeneration: The Level Study. *Brit. J. Ophthalmol* **2010**, *94*, 1611–1617.
- Tunon, J.; Ruiz-Moreno, J. M.; Martin-Ventura, J. L.; Blanco-Colio, L. M.; Lorenzo, O.; Egido, J. Cardiovascular Risk and Antiangiogenic Therapy for Age-Related Macular Degeneration. *Surv. Ophthalmol.* **2009**, *54*, 339–348.
- Alvarez, R. H.; Kantarjian, H. M.; Cortes, J. E. Biology of Platelet-Derived Growth Factor and Its Involvement in Disease. *Mayo Clin. Proc.* **2006**, *81*, 1241–1257.
- Jo, N.; Mailhos, C.; Ju, M. H.; Cheung, E.; Bradley, J.; Nishijima, K.; Robinson, G. S.; Adarnis, A. P.; Shima, D. T. Inhibition of Platelet-Derived Growth Factor B Signaling Enhances the Efficacy of Anti-vascular Endothelial Growth Factor Therapy in Multiple Models of Ocular Neovascularization. *Am. J. Pathol.* **2006**, *168*, 2036–2053.
- Green, L. S.; Jellinek, D.; Jenison, R.; Ostman, A.; Heldin, C. H.; Janjic, N. Inhibitory DNA Ligands to Platelet-Derived Growth Factor B-Chain. *Biochemistry* **1996**, *35*, 14413–14424.
- Biesecker, G.; Dihel, L.; Enney, K.; Bendele, R. A. Derivation of RNA Aptamer Inhibitors of Human Complement C5. *Immunopharmacology* **1999**, *42*, 219–230.
- Anderson, D. H.; Radeke, M. J.; Gallo, N. B.; Chapin, E. A.; Johnson, P. T.; Curletti, C. R.; Hancox, L. S.; Hu, J.; Ebricht, J. N.; Malek, G.; et al. The Pivotal Role of the Complement System in Aging and Age-Related Macular Degeneration: Hypothesis Re-visited. *Prog. Retin. Eye Res.* **2010**, *29*, 95–112.
- Rusconi, C. P.; Scardino, E.; Layzer, J.; Pitoc, G. A.; Ortel, T. L.; Monroe, D.; Sullenger, B. A. RNA Aptamers as Reversible Antagonists of Coagulation Factor IXa. *Nature* **2002**, *419*, 90–94.
- Cohen, M. G.; Purdy, D. A.; Rossi, J. S.; Grinfeld, L. R.; Myles, S. K.; Aberle, L. H.; Greenbaum, A. B.; Fry, E.; Chan, M. Y.; Tonkens, R. M.; et al. First Clinical Application of an Actively Reversible Direct Factor IXa Inhibitor as an Anticoagulation Strategy in Patients Undergoing Percutaneous Coronary Intervention. *Circulation* **2010**, *122*, 614–622.
- Diener, J. L.; Lagasse, H. A. D.; Duerschmied, D.; Merhi, Y.; Tanguay, J. F.; Hutabarat, R.; Gilbert, J.; Wagner, D. D.; Schaub, R. Inhibition of Von Willebrand Factor-Mediated



- Platelet Activation and Thrombosis by the Anti-Von Willebrand Factor A1-Domain Aptamer ARC1779. *J. Thromb. Haemostasis* **2009**, *7*, 1155–1162.
30. Lillicrap, D. Genotype/Phenotype Association in Von Willebrand Disease: Is the Glass Half Full or Empty? *J. Thromb. Haemostasis* **2009**, *7*, 65–70.
  31. Sadler, J. E.; Budde, U.; Eikenboom, J. C. J.; Favaloro, E. J.; Hill, F. G. H.; Holmberg, L.; Ingerslev, J.; Lee, C. A.; Lillicrap, D.; Mannucci, M.; et al. Update on the Pathophysiology and Classification of Von Willebrand Disease: A Report of the Subcommittee on Von Willebrand Factor. *J. Thromb. Haemostasis* **2006**, *4*, 2103–2114.
  32. Jilma, B.; Paulinska, P.; Jilma-Stohlwetz, P.; Gilbert, J. C.; Hutabarat, R.; Knobl, P. A Randomised Pilot Trial of the Anti-Von Willebrand Factor Aptamer ARC1779 in Patients with Type 2B Von Willebrand Disease. *Thromb. Haemostasis* **2010**, *104*, 563–570.
  33. Waters, E. K.; Richardson, J.; Schaub, R. G.; Kurz, J. C. Effect of NU172 and Bivalirudin on Ecarin Clotting Time in Human Plasma and Whole Blood. *J. Thromb Haemostasis* **2009**, *7*, 683.
  34. Waters, E. K.; Genga, R. M.; Schwartz, M. C.; Nelson, J. A.; Schaub, R. G.; Olson, K. A.; Kurz, J. C.; McGinness, K. E. Aptamer ARC19499 Mediates a Procoagulant Hemostatic Effect by Inhibiting Tissue Factor Pathway Inhibitor. *Blood* **2011**, *117*, 5514–5522.
  35. Bates, P. J.; Laber, D. A.; Miller, D. M.; Thomas, S. D.; Trent, J. O. Discovery and Development of the G-Rich Oligonucleotide AS1411 as a Novel Treatment for Cancer. *Exp. Mol. Pathol.* **2009**, *86*, 151–164.
  36. Hoellenriegel, J.; Zboralski, D.; Maasch, C.; Rosin, N. Y.; Wierda, W. G.; Keating, M. J.; Kruschinski, A.; Burger, J. A. The Spiegelmer NOX-A12, a Novel CXCL12 Inhibitor, Interferes with Chronic Lymphocytic Leukemia Cell Motility and Causes Chemosensitization. *Blood* **2014**, *123*, 1032–1039.
  37. Vater, A.; Klussmann, S. Toward Third-Generation Aptamers: Spiegelmers and Their Therapeutic Prospects. *Curr. Opin. Drug Discovery Dev.* **2003**, *6*, 253–261.
  38. Marasca, R.; Maffei, R. NOX-A12: Mobilizing CLL Away from Home. *Blood* **2014**, *123*, 952–953.
  39. Schwoebel, F.; van Eijk, L. T.; Zboralski, D.; Sell, S.; Buchner, K.; Maasch, C.; Purschke, W. G.; Humphrey, M.; Zollner, S.; Eulberg, D.; et al. The Effects of the Antihypertensive Spiegelmer NOX-H94 on Inflammation-Induced Anemia in Cynomolgus Monkeys. *Blood* **2013**, *121*, 2311–2315.
  40. Kulkarni, O.; Pawar, R. D.; Purschke, W.; Eulberg, D.; Selve, N.; Buchner, K.; Ninichuk, V.; Segerer, S.; Vielhauer, V.; Klussmann, S.; et al. Spiegelmer Inhibition of CCL2/MCP-1 Ameliorates Lupus Nephritis in MRL-(Fas)lpr Mice. *J. Am. Soc. Nephrol.* **2007**, *18*, 2350–2358.
  41. Ganz, T. Heparin, a Key Regulator of Iron Metabolism and Mediator of Anemia of Inflammation. *Blood* **2003**, *102*, 783–788.
  42. Ninichuk, V.; Clauss, S.; Kulkarni, O.; Schmid, H.; Segerer, S.; Radomska, E.; Eulberg, D.; Buchner, K.; Selve, N.; Klussmann, S.; et al. Late Onset of CC12 Blockade with the Spiegelmer mNOX-E36-3' PEG Prevents Glomerulosclerosis and Improves Glomerular Filtration Rate in db/db Mice. *Am. J. Pathol.* **2008**, *172*, 628–637.
  43. Gold, L.; Ayers, D.; Bertino, J.; Bock, C.; Bock, A.; Brody, E. N.; Carter, J.; Dalby, A. B.; Eaton, B. E.; Fitzwater, T.; et al. Aptamer-Based Multiplexed Proteomic Technology for Biomarker Discovery. *PLoS One* **2010**, *5*, e15004.
  44. Davies, D. R.; Gelinis, A. D.; Zhang, C.; Rohloff, J. C.; Carter, J. D.; O'Connell, D.; Waugh, S. M.; Wolk, S. K.; Mayfield, W. S.; Burgin, A. B.; et al. Unique Motifs and Hydrophobic Interactions Shape the Binding of Modified DNA Ligands to Protein Targets. *Proc. Natl. Acad. Sci. U.S.A.* **2012**, *109*, 19971–19976.
  45. Vaught, J. D.; Bock, C.; Carter, J.; Fitzwater, T.; Otis, M.; Schneider, D.; Rolando, J.; Waugh, S.; Wilcox, S. K.; Eaton, B. E. Expanding the Chemistry of DNA for *In Vitro* Selection. *J. Am. Chem. Soc.* **2010**, *132*, 4141–4151.
  46. Kimoto, M.; Yamashige, R.; Matsunaga, K.; Yokoyama, S.; Hirao, I. Generation of High-Affinity DNA Aptamers Using an Expanded Genetic Alphabet. *Nat. Biotechnol.* **2013**, *31*, 453–457.
  47. Park, N. J.; Wang, X. Q.; Diaz, A.; Goos-Root, D. M.; Bock, C.; Vaught, J. D.; Sun, W. M.; Strom, C. M. Measurement of Cetuximab and Panitumumab-Unbound Serum EGFR Extracellular Domain Using an Assay Based on Slow Off-Rate Modified Aptamer (SOMAmer) Reagents. *PLoS One* **2013**, *8*, e71703.
  48. Ostroff, R. M.; Bigbee, W. L.; Franklin, W.; Gold, L.; Mehan, M.; Miller, Y. E.; Pass, H. I.; Rom, W. N.; Siegfried, J. M.; Stewart, A.; et al. Unlocking Biomarker Discovery: Large Scale Application of Aptamer Proteomic Technology for Early Detection of Lung Cancer. *PLoS One* **2010**, *5*, e15003.
  49. Cruz-Toledo, J.; McKeague, M.; Zhang, X. R.; Giamberardino, A.; McConnell, E.; Francis, T.; DeRosa, M. C.; Dumontier, M. Aptamer Base: A Collaborative Knowledge Base To Describe Aptamers and SELEX Experiments. *Database* **2012**, *2012*, bas006.
  50. Chang, Y. C.; Kao, W. C.; Wang, W. Y.; Wang, W. Y.; Yang, R. B.; Peck, K. Identification and Characterization of Oligonucleotides That Inhibit Toll-like Receptor 2-Associated Immune Responses. *Faseb J.* **2009**, *23*, 3078–3088.
  51. Cheng, C. S.; Dong, J.; Yao, L. H.; Chen, A. J.; Jia, R. Q.; Huan, L. F.; Guo, J. L.; Shu, Y. L.; Zhang, Z. Q. Potent Inhibition of Human Influenza H5N1 Virus by Oligonucleotides Derived by SELEX. *Biochem. Biophys. Res. Commun.* **2008**, *366*, 670–674.
  52. Jeon, S. H.; Kayhan, B.; Ben-Yedidia, T.; Arnon, R. A DNA Aptamer Prevents Influenza Infection by Blocking the Receptor Binding Region of the Viral Hemagglutinin. *J. Biol. Chem.* **2004**, *279*, 48410–48419.
  53. Lao, Y. H.; Chiang, H. Y.; Yang, D. K.; Peck, K.; Chen, L. C. Selection of Aptamers Targeting the Sialic Acid Receptor of Hemagglutinin by Epitope-Specific SELEX. *Chem. Commun.* **2014**, *50*, 8719–8722.
  54. Waybrant, B.; Pearce, T. R.; Wang, P.; Sreevatsan, S.; Kokkoli, E. Development and Characterization of an Aptamer Binding Ligand of Fractalkine Using Domain Targeted SELEX. *Chem. Commun.* **2012**, *48*, 10043–10045.
  55. Bagalkot, V.; Farokhzad, O. C.; Langer, R.; Jon, S. An Aptamer–Doxorubicin Physical Conjugate as a Novel Targeted Drug-Delivery Platform. *Angew. Chem., Int. Ed.* **2006**, *45*, 8149–8152.
  56. Liu, Z.; Duan, J. H.; Song, Y. M.; Ma, J.; Wang, F. D.; Lu, X.; Yang, X. D. Novel HER2 Aptamer Selectively Delivers Cytotoxic Drug to HER2-Positive Breast Cancer Cells *In Vitro*. *J. Transl. Med.* **2012**, *10*, 148.
  57. Hu, Y.; Duan, J. H.; Zhan, Q. M.; Wang, F. D.; Lu, X.; Yang, X. D. Novel MUC1 Aptamer Selectively Delivers Cytotoxic Agent to Cancer Cells *In Vitro*. *PLoS One* **2012**, *7*, e31970.
  58. Shieh, Y. A.; Yang, S. J.; Wei, M. F.; Shieh, M. J. Aptamer-Based Tumor-Targeted Drug Delivery for Photodynamic Therapy. *ACS Nano* **2010**, *4*, 1433–1442.
  59. Zhou, C. S.; Jiang, Y. X.; Hou, S.; Ma, B. C.; Fang, X. H.; Li, M. L. Detection of Oncoprotein Platelet-Derived Growth Factor Using a Fluorescent Signaling Complex of an Aptamer and TOTO. *Anal. Bioanal. Chem.* **2006**, *384*, 1175–1180.
  60. Boyacioglu, O.; Stuart, C. H.; Kulik, G.; Gmeiner, W. H. Dimeric DNA Aptamer Complexes for High-Capacity-Targeted Drug Delivery Using pH-Sensitive Covalent Linkages. *Mol. Ther.—Nucleic Acids* **2013**, *2*, e107.
  61. Zhu, G. Z.; Zheng, J.; Song, E. Q.; Donovan, M.; Zhang, K. J.; Liu, C.; Tan, W. H. Self-Assembled, Aptamer-Tethered DNA Nanotrains for Targeted Transport of Molecular Drugs in Cancer Theranostics. *Proc. Natl. Acad. Sci. U.S.A.* **2013**, *110*, 7998–8003.
  62. Chang, M.; Yang, C. S.; Huang, D. M. Aptamer-Conjugated DNA Icosahedral Nanoparticles as a Carrier of Doxorubicin for Cancer Therapy. *ACS Nano* **2011**, *5*, 6156–6163.
  63. Shangguan, D.; Cao, Z. H.; Meng, L.; Mallikaratchy, P.; Sefah, K.; Wang, H.; Li, Y.; Tan, W. H. Cell-Specific Aptamer

- Probes for Membrane Protein Elucidation in Cancer Cells. *J. Proteome Res.* **2008**, *7*, 2133–2139.
64. Shangguan, D.; Li, Y.; Tang, Z. W.; Cao, Z. H. C.; Chen, H. W.; Mallikaratchy, P.; Sefah, K.; Yang, C. Y. J.; Tan, W. H. Aptamers Evolved from Live Cells as Effective Molecular Probes for Cancer Study. *Proc. Natl. Acad. Sci. U.S.A.* **2006**, *103*, 11838–11843.
  65. Chu, T. C.; Marks, J. W.; Lavery, L. A.; Faulkner, S.; Rosenblum, M. G.; Ellington, A. D.; Levy, M. Aptamer: Toxin Conjugates That Specifically Target Prostate Tumor Cells. *Cancer Res.* **2006**, *66*, 5989–5992.
  66. Huang, Y. F.; Shangguan, D. H.; Liu, H. P.; Phillips, J. A.; Zhang, X. L.; Chen, Y.; Tan, W. H. Molecular Assembly of an Aptamer–Drug Conjugate for Targeted Drug Delivery to Tumor Cells. *ChemBioChem* **2009**, *10*, 862–868.
  67. Wang, R. W.; Zhu, G. Z.; Mei, L.; Xie, Y.; Ma, H. B.; Ye, M.; Qing, F. L.; Tan, W. H. Automated Modular Synthesis of Aptamer–Drug Conjugates for Targeted Drug Delivery. *J. Am. Chem. Soc.* **2014**, *136*, 2731–2734.
  68. Xu, W. J.; Siddiqui, I. A.; Nihal, M.; Pilla, S.; Rosenthal, K.; Mukhtar, H.; Gong, S. Q. Aptamer-Conjugated and Doxorubicin-Loaded Unimolecular Micelles for Targeted Therapy of Prostate Cancer. *Biomaterials* **2013**, *34*, 5244–5253.
  69. Lupold, S. E.; Hicke, B. J.; Lin, Y.; Coffey, D. S. Identification and Characterization of Nuclease-Stabilized RNA Molecules That Bind Human Prostate Cancer Cells via the Prostate-Specific Membrane Antigen. *Cancer Res.* **2002**, *62*, 4029–4033.
  70. Farokhzad, O. C.; Cheng, J. J.; Teply, B. A.; Sherifi, I.; Jon, S.; Kantoff, P. W.; Richie, J. P.; Langer, R. Targeted Nanoparticle–Aptamer Bioconjugates for Cancer Chemotherapy *in Vivo*. *Proc. Natl. Acad. Sci. U.S.A.* **2006**, *103*, 6315–6320.
  71. Dhar, S.; Gu, F. X.; Langer, R.; Farokhzad, O. C.; Lippard, S. J. Targeted Delivery of Cisplatin to Prostate Cancer Cells by Aptamer Functionalized Pt(IV) Prodrug-PLGA-PEG Nanoparticles. *Proc. Natl. Acad. Sci. U.S.A.* **2008**, *105*, 17356–17361.
  72. Dhar, S.; Kolishetti, N.; Lippard, S. J.; Farokhzad, O. C. Targeted Delivery of a Cisplatin Prodrug for Safer and More Effective Prostate Cancer Therapy *in Vivo*. *Proc. Natl. Acad. Sci. U.S.A.* **2011**, *108*, 1850–1855.
  73. Kolishetti, N.; Dhar, S.; Valencia, P. M.; Lin, L. Q.; Karnik, R.; Lippard, S. J.; Langer, R.; Farokhzad, O. C. Engineering of Self-Assembled Nanoparticle Platform for Precisely Controlled Combination Drug Therapy. *Proc. Natl. Acad. Sci. U.S.A.* **2010**, *107*, 17939–17944.
  74. Guo, J. W.; Gao, X. L.; Su, L. N.; Xia, H. M.; Gu, G. Z.; Pang, Z. Q.; Jiang, X. G.; Yao, L.; Chen, J.; Chen, H. Z. Aptamer-Functionalized PEG-PLGA Nanoparticles for Enhanced Antiglioma Drug Delivery. *Biomaterials* **2011**, *32*, 8010–8020.
  75. Danhier, F.; Ansorena, E.; Silva, J. M.; Coco, R.; Le Breton, A.; Preat, V. PLGA-Based Nanoparticles: An Overview of Biomedical Applications. *J. Controlled Release* **2012**, *161*, 505–522.
  76. Knop, K.; Hoogenboom, R.; Fischer, D.; Schubert, U. S. Poly(ethylene glycol) in Drug Delivery: Pros and Cons as Well as Potential Alternatives. *Angew. Chem., Int. Ed.* **2010**, *49*, 6288–6308.
  77. Torchilin, V. P. Recent Advances with Liposomes as Pharmaceutical Carriers. *Nat. Rev. Drug Discovery* **2005**, *4*, 145–160.
  78. Samad, A.; Sultana, Y.; Aqil, M. Liposomal Drug Delivery Systems: An Update Review. *Curr. Drug Delivery* **2007**, *4*, 297–305.
  79. Cao, Z. H.; Tong, R.; Mishra, A.; Xu, W. C.; Wong, G. C. L.; Cheng, J. J.; Lu, Y. Reversible Cell-Specific Drug Delivery with Aptamer-Functionalized Liposomes. *Angew. Chem., Int. Ed.* **2009**, *48*, 6494–6498.
  80. Xing, H.; Tang, L.; Yang, X. J.; Hwang, K.; Wang, W. D.; Yin, Q.; Wong, N. Y.; Dobrucki, L. W.; Yasui, N.; Katzenellenbogen, J. A.; et al. Selective Delivery of an Anticancer Drug with Aptamer-Functionalized Liposomes to Breast Cancer Cells *in Vitro* and *in Vivo*. *J. Mater. Chem. B* **2013**, *1*, 5288–5297.
  81. Xie, L. L.; Tong, W. J.; Yu, D. H.; Xu, J. Q.; Li, J.; Gao, C. Y. Bovine Serum Albumin Nanoparticles Modified with Multilayers and Aptamers for pH-Responsive and Targeted Anti-cancer Drug Delivery. *J. Mater. Chem.* **2012**, *22*, 6053–6060.
  82. Wu, Y. R.; Sefah, K.; Liu, H. P.; Wang, R. W.; Tan, W. H. DNA Aptamer-Micelle as an Efficient Detection/Delivery Vehicle toward Cancer Cells. *Proc. Natl. Acad. Sci. U.S.A.* **2010**, *107*, 5–10.
  83. Li, L. L.; Xie, M. Y.; Wang, J.; Li, X. Y.; Wang, C.; Yuan, Q.; Pang, D. W.; Lu, Y.; Tan, W. H. A Vitamin-Responsive Mesoporous Nanocarrier with DNA Aptamer-Mediated Cell Targeting. *Chem. Commun.* **2013**, *49*, 5823–5825.
  84. McNamara, J. O.; Andrechek, E. R.; Wang, Y.; D Viles, K.; Rempel, R. E.; Gilboa, E.; Sullenger, B. A.; Giangrande, P. H. Cell Type-Specific Delivery of siRNAs with Aptamer–siRNA Chimeras. *Nat. Biotechnol.* **2006**, *24*, 1005–1015.
  85. Lai, W. Y.; Wang, W. Y.; Chang, Y. C.; Chang, C. J.; Yang, P. C.; Peck, K. Synergistic Inhibition of Lung Cancer Cell Invasion, Tumor Growth and Angiogenesis Using Aptamer–siRNA Chimeras. *Biomaterials* **2014**, *35*, 2905–2914.
  86. Dai, F. R.; Zhang, Y.; Zhu, X.; Shan, N. C.; Chen, Y. X. Anticancer Role of MUC1 Aptamer–miR-29b Chimera in Epithelial Ovarian Carcinoma Cells through Regulation of PTEN Methylation. *Target Oncol.* **2012**, *7*, 217–225.
  87. Esposito, C. L.; Cerchia, L.; Catuogno, S.; De Vita, G.; Dassisti, J. P.; Santamaria, G.; Swiderski, P.; Condorelli, G.; Giangrande, P. H.; de Franciscis, V. Multifunctional Aptamer–miRNA Conjugates for Targeted Cancer Therapy. *Mol. Ther.* **2014**, *22*, 1151–1163.
  88. Ferreira, C. S. M.; Matthews, C. S.; Missailidis, S. DNA Aptamers That Bind to MUC1 Tumour Marker: Design and Characterization of MUC1-Binding Single-Stranded DNA Aptamers. *Tumor Biol.* **2006**, *27*, 289–301.
  89. Garzon, R.; Liu, S. J.; Fabbri, M.; Liu, Z. F.; Heaphy, C. E. A.; Callegari, E.; Schwind, S.; Pang, J. X.; Yu, J. H.; Muthusamy, N.; et al. MicroRNA-29b Induces Global DNA Hypomethylation and Tumor Suppressor Gene Reexpression in Acute Myeloid Leukemia by Targeting Directly DNMT3A and 3B and Indirectly DNMT1. *Blood* **2009**, *113*, 6411–6418.
  90. Dai, F. R.; Zhang, Y.; Zhu, X.; Shan, N. C.; Chen, Y. X. The Anti-chemoresistant Effect and Mechanism of MUC1 Aptamer–miR-29b Chimera in Ovarian Cancer. *Gynecol. Oncol.* **2013**, *131*, 451–459.
  91. Cerchia, L.; Esposito, C. L.; Camorani, S.; Rienzo, A.; Stasio, L.; Insabato, L.; Affuso, A.; de Franciscis, V. Targeting Axl with an High-Affinity Inhibitory Aptamer. *Mol. Ther.* **2012**, *20*, 2291–2303.
  92. Boyerinas, B.; Park, S. M.; Hau, A.; Murmann, A. E.; Peter, M. E. The Role of Let-7 in Cell Differentiation and Cancer. *Endocr-Relat. Cancer* **2010**, *17*, F19–F36.
  93. Ni, X. H.; Zhang, Y. G.; Ribas, J.; Chowdhury, W. H.; Castanares, M.; Zhang, Z. W.; Laiho, M.; DeWeese, T. L.; Lupold, S. E. Prostate-Targeted Radiosensitization via Aptamer–shRNA Chimeras in Human Tumor Xenografts. *J. Clin. Invest.* **2011**, *121*, 2383–2390.
  94. Beisel, C. L.; Bayer, T. S.; Hoff, K. G.; Smolke, C. D. Model-Guided Design of Ligand-Regulated RNAi for Programmable Control of Gene Expression. *Mol. Syst. Biol.* **2008**, *4*, 224.
  95. Dassisti, J. P.; Liu, X. Y.; Thomas, G. S.; Whitaker, R. M.; Thiel, K. W.; Stockdale, K. R.; Meyerholz, D. K.; McCaffrey, A. P.; McNamara, J. O.; Giangrande, P. H. Systemic Administration of Optimized Aptamer–siRNA Chimeras Promotes Regression of PSMA-Expressing Tumors. *Nat. Biotechnol.* **2009**, *27*, 839–846.
  96. Yang, J.; Xie, S. X.; Huang, Y. L.; Ling, M.; Liu, J. H.; Ran, Y. L.; Wang, Y. L.; Thrasher, J. B.; Berkland, C.; Li, B. Y. Prostate-Targeted Biodegradable Nanoparticles Loaded with Androgen Receptor Silencing Constructs Eradicate Xenograft Tumors in Mice. *Nanomedicine* **2012**, *7*, 1297–1309.
  97. Li, L. Y.; Hou, J. J.; Liu, X. J.; Guo, Y. J.; Wu, Y.; Zhang, L. H.; Yang, Z. J. Nucleolin-Targeting Liposomes Guided by Aptamer AS1411 for the Delivery of siRNA for the

- Treatment of Malignant Melanomas. *Biomaterials* **2014**, *35*, 3840–3850.
98. Tang, Z. W.; Shangguan, D.; Wang, K. M.; Shi, H.; Sefah, K.; Mallikratchy, P.; Chen, H. W.; Li, Y.; Tan, W. H. Selection of Aptamers for Molecular Recognition and Characterization of Cancer Cells. *Anal. Chem.* **2007**, *79*, 4900–4907.
  99. Mallikratchy, P.; Tang, Z. W.; Kwame, S.; Meng, L.; Shangguan, D. H.; Tan, W. H. Aptamer Directly Evolved from Live Cells Recognizes Membrane Bound Immunoglobulin Heavy Mu Chain in Burkitt's Lymphoma Cells. *Mol. Cell Proteomics* **2007**, *6*, 2230–2238.
  100. Shi, H.; Tang, Z. W.; Kim, Y.; Nie, H. L.; Huang, Y. F.; He, X. X.; Deng, K.; Wang, K. M.; Tan, W. H. *In Vivo* Fluorescence Imaging of Tumors Using Molecular Aptamers Generated by Cell-SELEX. *Chem.—Asian J.* **2010**, *5*, 2209–2213.
  101. Shi, H.; Cui, W. S.; He, X. X.; Guo, Q. P.; Wang, K. M.; Ye, X. S.; Tang, J. L. Whole Cell-SELEX Aptamers for Highly Specific Fluorescence Molecular Imaging of Carcinomas *in Vivo*. *PLoS One* **2013**, *8*, e70476.
  102. Lubin, A. A.; Plaxco, W. F. Folding-Based Electrochemical Biosensors: The Case for Responsive Nucleic Acid Architectures. *Acc. Chem. Res.* **2010**, *43*, 496–505.
  103. Cheng, A. K. H.; Su, H. P.; Wang, A.; Yu, H. Z. Aptamer-Based Detection of Epithelial Tumor Marker Mucin 1 with Quantum Dot-Based Fluorescence Readout. *Anal. Chem.* **2009**, *81*, 6130–6139.
  104. Chi, C. W.; Lao, Y. H.; Li, Y. S.; Chen, L. C. A Quantum Dot—Aptamer Beacon Using a DNA Intercalating Dye as the FRET Reporter: Application to Label-Free Thrombin Detection. *Biosens. Bioelectron.* **2011**, *26*, 3346–3352.
  105. Shi, H.; He, X. X.; Wang, K. M.; Wu, X.; Ye, X. S.; Guo, Q. P.; Tan, W. H.; Qing, Z. H.; Yang, X. H.; Zhou, B. Activatable Aptamer Probe for Contrast-Enhanced *In Vivo* Cancer Imaging Based on Cell Membrane Protein-Triggered Conformation Alteration. *Proc. Natl. Acad. Sci. U.S.A.* **2011**, *108*, 3900–3905.
  106. Shokrollahi, H. Contrast Agents for MRI. *Mater. Sci. Eng., C* **2013**, *33*, 4485–4497.
  107. Hu, H.; Dai, A. T.; Sun, J.; Li, X. Y.; Gao, F. H.; Wu, L. Z.; Fang, Y.; Yang, H.; An, L.; Wu, H. X.; et al. Aptamer-Conjugated  $Mn_3O_4@SiO_2$  Core—Shell Nanoparticles for Targeted Magnetic Resonance Imaging. *Nanoscale* **2013**, *5*, 10447–10454.
  108. Kim, B.; Yang, J.; Hwang, M.; Choi, J.; Kim, H. O.; Jang, E.; Lee, J. H.; Ryu, S. H.; Suh, J. S.; Huh, Y. M.; et al. Aptamer-Modified Magnetic Nanoprobe for Molecular MR Imaging of VEGFR2 on Angiogenic Vasculature. *Nanoscale Res. Lett.* **2013**, *8*, 1–10.
  109. Charlton, J.; Sennello, J.; Smith, D. *In Vivo* Imaging of Inflammation Using an Aptamer Inhibitor of Human Neutrophil Elastase. *Chem. Biol.* **1997**, *4*, 809–816.
  110. Hicke, B. J.; Marion, C.; Chang, Y. F.; Gould, T.; Lynott, C. K.; Parma, D.; Schmidt, P. G.; Warren, S. Tenascin-C Aptamers Are Generated Using Tumor Cells and Purified Protein. *J. Biol. Chem.* **2001**, *276*, 48644–48654.
  111. Borbas, K. E.; Ferreira, C. S. M.; Perkins, A.; Bruce, J. I.; Missailidis, S. Design and Synthesis of Mono- and Multimeric Targeted Radiopharmaceuticals Based on Novel Cyclen Ligands Coupled to Anti-MUC1 Aptamers for the Diagnostic Imaging and Targeted Radiotherapy of Cancer. *Bioconjugate Chem.* **2007**, *18*, 1205–1212.
  112. Bagalkot, V.; Zhang, L.; Levy-Nissenbaum, E.; Jon, S.; Kantoff, P. W.; Langer, R.; Farokhzad, O. C. Quantum Dot—Aptamer Conjugates for Synchronous Cancer Imaging, Therapy, and Sensing of Drug Delivery Based on Bioluminescence Resonance Energy Transfer. *Nano Lett.* **2007**, *7*, 3065–3070.
  113. Jalalian, S. H.; Taghdisi, S. M.; Hamedani, N. S.; Kalat, S. A. M.; Lavaee, P.; ZandKarimi, M.; Ghows, N.; Jaafari, M. R.; Naghibi, S.; Danesh, N. M.; et al. Epirubicin Loaded Super Paramagnetic Iron Oxide Nanoparticle—Aptamer Bioconjugate for Combined Colon Cancer Therapy and Imaging *in Vivo*. *Eur. J. Pharm. Sci.* **2013**, *50*, 191–197.
  114. Savla, R.; Taratula, O.; Garbuzenko, O.; Minko, T. Tumor Targeted Quantum Dot—Mucin 1 Aptamer—Doxorubicin Conjugate for Imaging and Treatment of Cancer. *J. Controlled Release* **2011**, *153*, 16–22.
  115. Kraemer, S.; Vaught, J. D.; Bock, C.; Gold, L.; Katilius, E.; Keeney, T. R.; Kim, N.; Saccomano, N. A.; Wilcox, S. K.; Zichi, D.; et al. From SOMAmer-Based Biomarker Discovery to Diagnostic and Clinical Applications: A SOMAmer-Based, Streamlined Multiplex Proteomic Assay. *PLoS One* **2011**, *6*, e26332.
  116. Sefah, K.; Shangguan, D.; Xiong, X. L.; O'Donoghue, M. B.; Tan, W. H. Development of DNA Aptamers Using Cell-SELEX. *Nat. Protoc.* **2010**, *5*, 1169–1185.
  117. Wang, C. W.; Chung, W. H.; Cheng, Y. F.; Ying, N. W.; Peck, K.; Chen, Y. T.; Hung, S. I. A New Nucleic Acid-Based Agent Inhibits Cytotoxic T Lymphocyte-Mediated Immune Disorders. *J. Allergy Clin. Immunol.* **2013**, *132*, 713–722.
  118. Mi, J.; Liu, Y. M.; Rabbani, Z. N.; Yang, Z. G.; Urban, J. H.; Sullenger, B. A.; Clary, B. M. *In Vivo* Selection of Tumor-Targeting RNA Motifs. *Nat. Chem. Biol.* **2010**, *6*, 22–24.
  119. Cheng, C. S.; Chen, Y. H.; Lennox, K. A.; Behlke, M. A.; Davidson, B. L. *In Vivo* SELEX for Identification of Brain-Penetrating Aptamers. *Mol. Ther.—Nucleic Acids* **2013**, *2*, e67.
  120. Martin, D. F.; Klein, M.; Haller, J.; Adamis, A.; Gragoudas, E.; Miller, J.; Blumenkrantz, M.; Goldberg, M.; Yannuzzi, L.; Henninger, D.; et al. Preclinical and Phase 1A Clinical Evaluation of an Anti-VEGF PEGylated Aptamer (EYE001) for the Treatment of Exudative Age-Related Macular Degeneration. *Retina* **2002**, *22*, 143–152.
  121. Ireson, C. R.; Kelland, L. R. Discovery and Development of Anticancer Aptamers. *Mol. Cancer Ther.* **2006**, *5*, 2957–2962.
  122. Akira, S.; Uematsu, S.; Takeuchi, O. Pathogen Recognition and Innate Immunity. *Cell* **2006**, *124*, 783–801.
  123. Wang, D. Q.; Bhagat, L.; Yu, D.; Zhu, F. G.; Tang, J. X.; Kandimalla, E. R.; Agrawal, S. Oligodeoxyribonucleotide-Based Antagonists for Toll-like Receptors 7 and 9. *J. Med. Chem.* **2009**, *52*, 551–558.
  124. Yu, D.; Wang, D. Q.; Zhu, F. G.; Bhagat, L.; Dai, M. R.; Kandimalla, E. R.; Agrawal, S. Modifications Incorporated in CPG Motifs of Oligodeoxynucleotides Lead to Antagonist Activity of Toll-like Receptors 7 and 9. *J. Med. Chem.* **2009**, *52*, 5108–5114.
  125. Shukla, S.; Sumaria, C. S.; Pradeepkumar, P. I. Exploring Chemical Modifications for siRNA Therapeutics: A Structural and Functional Outlook. *ChemMedChem* **2010**, *5*, 328–349.
  126. Goldberg, M. S.; Xing, D. Y.; Ren, Y.; Orsulic, S.; Bhatia, S. N.; Sharp, P. A. Nanoparticle-Mediated Delivery of siRNA Targeting Parp1 Extends Survival of Mice Bearing Tumors Derived from Brca1-Deficient Ovarian Cancer Cells. *Proc. Natl. Acad. Sci. U.S.A.* **2011**, *108*, 745–750.
  127. Griffin, L. C.; Tidmarsh, G. F.; Bock, L. C.; Toole, J. J.; Leung, L. L. K. *In Vivo* Anticoagulant Properties of a Novel Nucleotide-Based Thrombin Inhibitor and Demonstration of Regional Anticoagulation in Extracorporeal Circuits. *Blood* **1993**, *81*, 3271–3276.
  128. Moore, M. D.; Cookson, J.; Coventry, V. K.; Sproat, B.; Rabe, L.; Cranston, R. D.; McGowan, I.; James, W. Protection of HIV Neutralizing Aptamers against Rectal and Vaginal Nucleases Implications for RNA-Based Therapeutics. *J. Biol. Chem.* **2011**, *286*, 2526–2535.
  129. Healy, J. M.; Lewis, S. D.; Kurz, M.; Boomer, R. M.; Thompson, K. M.; Wilson, C.; McCauley, T. G. Pharmacokinetics and Biodistribution of Novel Aptamer Compositions. *Pharm. Res.* **2004**, *21*, 2234–2246.
  130. Ruckman, J.; Green, L. S.; Beeson, J.; Waugh, S.; Gillette, W. L.; Henninger, D. D.; Claesson-Welsh, L.; Janjic, N. 2'-Fluoropyrimidine RNA-Based Aptamers to the 165-Amino Acid Form of Vascular Endothelial Growth Factor (VEGF(165)): Inhibition of Receptor Binding and VEGF-Induced Vascular Permeability through Interactions Requiring the Exon 7-Encoded Domain. *J. Biol. Chem.* **1998**, *273*, 20556–20567.
  131. Ortigao, J. F.; Rosch, H.; Selter, H.; Frohlich, A.; Lorenz, A.; Montenarh, M.; Seliger, H. Antisense Effect of

- Oligodeoxynucleotides with Inverted Terminal Internucleotidic Linkages: A Minimal Modification Protecting against Nucleolytic Degradation. *Antisense Res. Dev.* **1992**, *2*, 129–146.
132. Bouchard, P. R.; Hutabarat, R. M.; Thompson, K. M. Discovery and Development of Therapeutic Aptamers. *Annu. Rev. Pharmacol.* **2010**, *50*, 237–257.
133. Gu, F.; Zhang, L.; Teply, B. A.; Mann, N.; Wang, A.; Radovic-Moreno, A. F.; Langer, R.; Farokhzad, O. C. Precise Engineering of Targeted Nanoparticles by Using Self-Assembled Biointegrated Block Copolymers. *Proc. Natl. Acad. Sci. U.S.A.* **2008**, *105*, 2586–2591.
134. Jain, R. K.; Stylianopoulos, T. Delivering Nanomedicine to Solid Tumors. *Nat. Rev. Clin. Oncol.* **2010**, *7*, 653–664.
135. Tang, L.; Gabrielson, N. P.; Uckun, F. M.; Fan, T. M.; Cheng, J. J. Size-Dependent Tumor Penetration and *In Vivo* Efficacy of Monodisperse Drug–Silica Nanoconjugates. *Mol. Pharmaceutics* **2013**, *10*, 883–892.
136. Chauhan, V. P.; Jain, R. K. Strategies for Advancing Cancer Nanomedicine. *Nat. Mater.* **2013**, *12*, 958–962.
137. Lao, Y. H.; Peck, K.; Chen, L. C. Enhancement of Aptamer Microarray Sensitivity through Spacer Optimization and Avidity Effect. *Anal. Chem.* **2009**, *81*, 1747–1754.
138. Godsey, M. E.; Suryaprakash, S.; Leong, K. W. Materials Innovation for Co-delivery of Diverse Therapeutic Cargos. *RSC Adv.* **2013**, *3*, 24794–24811.
139. Santulli-Marotto, S.; Nair, S. K.; Rusconi, C.; Sullenger, B.; Gilboa, E. Multivalent RNA Aptamers That Inhibit CTLA-4 and Enhance Tumor Immunity. *Cancer Res.* **2003**, *63*, 7483–7489.
140. Herrmann, A.; Priceman, S. J.; Kujawski, M.; Xin, H.; Cherryholmes, G. A.; Zhang, W.; Zhang, C. Y.; Lahtz, C.; Kowolik, C.; Forman, S. J.; et al. CTLA4 Aptamer Delivers STAT3 siRNA to Tumor-Associated and Malignant T Cells. *J. Clin. Invest.* **2014**, *124*, 2977–2987.
141. Oney, S.; Lam, R. T. S.; Bompiani, K. M.; Blake, C. M.; Quick, G.; Heidel, J. D.; Liu, J. Y. C.; Mack, B. C.; Davis, M. E.; Leong, K. W.; et al. Development of Universal Antidotes To Control Aptamer Activity. *Nat. Med.* **2009**, *15*, 1224–1228.